

Metropolis–Hastings with Scalable Subsampling

Estevão Prado, Christopher Nemeth* and Chris Sherlock

School of Mathematical Sciences, Lancaster University, UK

July 30, 2024

Abstract

The Metropolis–Hastings (MH) algorithm is one of the most widely used Markov Chain Monte Carlo schemes for generating samples from Bayesian posterior distributions. The algorithm is asymptotically exact, flexible and easy to implement. However, in the context of Bayesian inference for large datasets, evaluating the likelihood on the full data for thousands of iterations until convergence can be prohibitively expensive. This paper introduces a new subsample MH algorithm that satisfies detailed balance with respect to the target posterior and utilises control variates to enable exact, efficient Bayesian inference on datasets with large numbers of observations. Through theoretical results, simulation experiments and real-world applications on certain generalised linear models, we demonstrate that our method requires substantially smaller subsamples and is computationally more efficient than the standard MH algorithm and other exact subsample MH algorithms.

Keywords: Markov Chain Monte Carlo, scalable Metropolis–Hastings algorithm, control variates, subsampling, big data.

1 Introduction

In the Bayesian framework, the posterior distribution of the model parameters contains all information needed for inference, but even with simple models, the posterior is generally known only up to a constant of proportionality. Markov Chain Monte Carlo (MCMC; [Robert et al., 1999](#); [Brooks et al., 2011](#)) is a class of simulation methods commonly used in Bayesian statistics to sample from posterior distributions. At the core of MCMC methods is the Metropolis–Hastings (MH) algorithm, which proposes at each iteration a new parameter value and then decides whether or not to accept it. The acceptance decision requires the evaluation of the full (unnormalised) posterior density evaluated at the proposed parameter and this in turn requires the evaluation of every single term in the likelihood. In this big-data era, where datasets consist of millions or even billions of data points, each likelihood evaluation is computationally expensive and it becomes infeasible to repeat this at every iteration, as required by the standard MH algorithm.

Optimisation-based algorithms, such as variational and Laplace approximations ([Raj et al., 2014](#); [Yogatama et al., 2014](#); [Andersen et al., 2018](#); [Winter et al., 2024](#)), are still feasible, but these are inexact. In this context, a new class of MCMC methods has gained attention more recently: *scalable MCMC* algorithms; see [Fearnhead et al. \(2024\)](#) for a recent review. In an attempt to alleviate the computational burden of performing traditional MCMC sampling on large datasets, some of the works in the scalable MCMC literature propose splitting the data

*The author was supported by EPSRC grants EP/V022636/1 and EP/Y028783/1.

into partitions and then, in parallel, performing posterior sampling on each partition across multiple CPUs. This approach is called ‘divide-and-conquer’, as the data are divided into multiple disjoint subsamples, and the final posterior is obtained by combining the subposteriors from each subsample. One of the challenges related to this approach is to efficiently combine the subposteriors in cases where the target distribution is non-Gaussian; see, for example, Neiswanger et al. (2013); Scott et al. (2016); Nemeth and Sherlock (2018); Vyner et al. (2023); Trojan et al. (2024).

Another avenue to reduce the computational cost of running MCMC algorithms on datasets with large number of observations utilises data subsampling (Maclaurin and Adams, 2014; Korattikara et al., 2014; Bardenet et al., 2014; Liu et al., 2015; Bardenet et al., 2017; Yuan and Wang, 2024). In contrast to the divide-and-conquer approach, subsampling-based MCMC methods speed up posterior sampling by running a single MCMC algorithm and using a random subsample of the data at each iteration. For instance, Quiroz et al. (2018a) propose a Metropolis-based MCMC algorithm that builds upon the pseudo-marginal approach (Beaumont, 2003; Andrieu and Roberts, 2009) and control variates (Ripley, 2009). The MH acceptance ratio is replaced with an approximation based on subsamples. To control the error introduced by this approximation, the MH ratio needs to be bias-corrected. Consequently, the algorithm is no longer exact, as the invariant distribution of the Markov chain is a perturbed version of the true posterior.

There are also subsample MCMC methods that are constructed in such a way that the invariant distribution of the resulting Markov chain is the true posterior distribution. All of these methods require that the full likelihood is a product of terms (typically, one term for each data point) and require some assumptions on the individual terms in the product. Subject to these constraints, only a random subsample of the terms needs to be evaluated at any given iteration of the MCMC algorithm. For instance, Maclaurin and Adams (2014) assume that for each observation there exists a strictly positive lower bound on the log-likelihood that accumulates tractably when summed over many observations; it then augments the parameter space using Bernoulli latent variables. Cornish et al. (2019) and Zhang et al. (2020) are less restrictive and do not augment the state space. Both of these algorithms replace the Metropolis–Hastings acceptance ratio with an alternative that uses a small number of subsamples and, hence, has a high variance. Cornish et al. (2019) uses control variates to reduce this variance, whilst Zhang et al. (2020) incorporates an additional parameter to mitigate the variance’s deleterious effect on the acceptance rate.

In this paper, we propose a new exact subsample MH algorithm that makes use of control variates and subsampling and produces a Markov chain that satisfies detailed balance with respect to the true posterior. The criterion (3) looks at the difference in log-likelihoods at the current and proposed values. It requires that the discrepancy between this difference and the estimate of the difference suggested by the control variates can be bounded by a product of a function of the parameters and a function of the data value. We establish general bounds that are typically much tighter than those considered in previous works, especially when the dimension, d , of the parameter vector is moderate or large. Specialising to regression models, we derive specific, tight bounds for three generalised linear models (GLMs) including the logistic regression model considered in previous works. More broadly, we establish that our algorithm is optimal within a particular class of subsample algorithms. All of this leads to a substantial speed-up in the posterior sampling. We also conduct an asymptotic analysis comparing our proposed bounds with previous approaches, demonstrating theoretically and empirically that the computational cost of using our bounds is at least a factor of $d^{1/2}$ better than previous bounds.

This paper is organised as follows. Section 2 introduces our algorithm and illustrates why it

targets the correct posterior. Section 3 discusses related works and issues with the existing subsample-based MH algorithms. Section 4 presents the general forms of the much tighter bounds we propose for the log-likelihood differences, as well as theoretical results on the exactness and optimality of our proposed algorithm and guidance on its tuning. The proofs of the results in this section are deferred to Appendix A. Sections 5 and 6 present simulation experiments and real-world applications using the logistic, probit and Poisson regression models, where our proposed method is compared against the equivalent Metropolis–Hastings algorithm and other subsample-based MH algorithms. Finally, Section 7 concludes with a discussion. Additional simulation experiments, asymptotic analyses comparing the new and existing bounds and results related to the acceptance rate of the proposed algorithms are presented in Appendices B, C and D.

2 Metropolis–Hastings with Scalable Subsampling

We are interested in sampling from a posterior distribution with density $\pi(\theta|y)$, where $\theta \in \mathcal{X} \subseteq \mathbb{R}^d$ denotes the parameter vector and $y = (y_1, \dots, y_n)$ are the observed data. Assuming a prior $p(\theta)$, and data that are conditionally independent with log likelihood terms $\ell_i(\theta) := \log p(y_i|\theta)$, the posterior density is

$$\pi(\theta|y) \propto p(\theta) \prod_{i=1}^n p(y_i|\theta) \equiv p(\theta)p(y_{1:n}|\theta) = p(\theta) \exp \left[\sum_{i=1}^n \ell_i(\theta) \right].$$

Given a current value, θ , and a proposal density, $q(\theta'|\theta)$, the Metropolis–Hastings acceptance probability is $1 \wedge [q(\theta|\theta')\pi(\theta'|y)/\{q(\theta'|\theta)\pi(\theta|y)\}]$. The contribution of the computationally expensive likelihood to this ratio is

$$\exp \left[\sum_{i=1}^n \{\ell_i(\theta') - \ell_i(\theta)\} \right].$$

To allow us to subsample terms from this sum whilst controlling the variance of the subsequent estimator, we create a deterministic approximation, called a control variate, for each difference, $\ell_i(\theta') - \ell_i(\theta)$. Let $\hat{\theta} \in \mathcal{X}$ be (ideally, but for strict correctness of the algorithm, not necessarily) close to the posterior mode. We choose control variates to be the approximations to $\ell_i(\theta') - \ell_i(\theta)$ that arise from first- and second-order Taylor expansion of ℓ_i about $\hat{\theta}$:

$$r_i^{(1)}(\theta, \theta'; \hat{\theta}) := (\theta' - \theta)^\top g_i(\hat{\theta}), \tag{1}$$

$$r_i^{(2)}(\theta, \theta'; \hat{\theta}) := (\theta' - \theta)^\top g_i(\hat{\theta}) + (\theta' - \theta)^\top H_i(\hat{\theta}) \left\{ \frac{1}{2}(\theta' + \theta) - \hat{\theta} \right\}, \tag{2}$$

where $g_i(\theta) = \nabla \ell_i(\theta)$ is the gradient of the log-likelihood and $H_i(\theta) = \nabla \nabla^\top \ell_i(\theta)$ is the Hessian. Whichever control variate, $k \in \{1, 2\}$, is used, our algorithm requires the existence of bounds $M^{(k)}(\theta, \theta') \geq 0$ and $c_1^{(k)}, \dots, c_n^{(k)} > 0$ such that $M^{(k)}(\theta, \theta') = M^{(k)}(\theta', \theta)$ for all $\theta, \theta' \in \mathcal{X}$ and

$$|\ell_i(\theta') - \ell_i(\theta) - r_i^{(k)}(\theta, \theta'; \hat{\theta})| \leq c_i^{(k)} M^{(k)}(\theta, \theta'). \tag{3}$$

In the following, for notational convenience, we drop the superscript (k) from $r_i^{(k)}(\theta, \theta'; \hat{\theta})$, $c_i^{(k)}$ and $M^{(k)}(\theta, \theta')$ and use the notation $r_i(\theta, \theta'; \hat{\theta})$, c_i , $M(\theta, \theta')$, respectively. Such bounds for logistic regression and robust linear regression models when $k = 1, 2$ are given in Cornish et al. (2019). In Section 4.2, we provide much-improved bounds for logistic, probit and a form of

Poisson regression. We define the difference between the control variate and the truth to be

$$\Delta_i := r_i(\theta, \theta'; \widehat{\theta}) - \{\ell_i(\theta') - \ell_i(\theta)\}, \quad (4)$$

and for $\gamma \in [0, 1]$ and we introduce the functions ϕ_i and ϕ'_i for $i = 1, \dots, n$ which are chosen to satisfy the following properties for all $\theta, \theta' \in \mathcal{X}$:

$$\text{F1: } 0 \leq \phi_i \leq c_i M(\theta, \theta').$$

$$\text{F2: } 0 \leq \phi'_i \leq c_i M(\theta, \theta').$$

$$\text{F3: } \phi_i - \phi'_i = \Delta_i.$$

The assumptions on ϕ_i and ϕ'_i ensure that these are bounded, non-negative functions whose difference is exactly the quantity of interest and which can be used as the expectations of Poisson random variables that can be sampled via Poisson thinning. In this paper, we choose

$$\phi_i = \gamma \max[0, \Delta_i] + (1 - \gamma) \{c_i M(\theta, \theta') + \min[0, \Delta_i]\}. \quad (5)$$

We also define the equivalent quantity when $\theta \leftrightarrow \theta'$ are interchanged:

$$\phi'_i = \gamma \max[0, \Delta'_i] + (1 - \gamma) \{c_i M(\theta', \theta) + \min[0, \Delta'_i]\}, \quad (6)$$

where $\Delta'_i = r_i(\theta', \theta; \widehat{\theta}) - \{\ell_i(\theta) - \ell_i(\theta')\} = -\Delta_i$, since $r_i(\theta', \theta; \widehat{\theta}) = -r_i(\theta, \theta'; \widehat{\theta})$ for both $r^{(1)}$ and $r^{(2)}$. From (3) and (4), both the multiplicand of γ and that of $1 - \gamma$ in (5) are between 0 and $c_i M(\theta, \theta')$, proving F1, and, by an analogous argument since $M(\theta, \theta') = M(\theta', \theta)$, F2. Since $\max[0, -\Delta_i] = -\min[0, \Delta_i]$ and $\min[0, -\Delta_i] = -\max[0, \Delta_i]$, F3 holds because $\max[0, \Delta_i] + \min[0, \Delta_i] = 0 + \Delta_i = \Delta_i$. Whilst our algorithm is valid for any $\gamma \in [0, 1]$, we show in Section 4.1 that it is always most efficient when $\gamma = 0$.

The non-negativity in F1 and F2 permits us to complete the set-up for our algorithm through the independent auxiliary variables

$$S_i \sim \text{Pois}(\phi_i), \quad i = 1, \dots, n. \quad (7)$$

S_i will be the number of times the i th likelihood term appears in our acceptance ratio. When ϕ_i is sufficiently small, this is very likely to be 0. From F3,

$$\frac{p(s_i | \theta', \theta)}{p(s_i | \theta, \theta')} = \frac{\exp(-\phi'_i) \phi_i'^{s_i} / s_i!}{\exp(-\phi_i) \phi_i^{s_i} / s_i!} = \exp(\Delta_i) \frac{\phi_i'^{s_i}}{\phi_i^{s_i}}.$$

Let $s := (s_1, \dots, s_n)$ and write $p(s | \theta, \theta') := \prod_{i=1}^n p(s_i | \theta, \theta')$. If the Metropolis–Hastings proposal density is $q(\theta' | \theta)$, detailed balance holds with respect to $\pi(\theta)$ if the probability of accepting θ' satisfies

$$\pi(\theta) q(\theta' | \theta) p(s | \theta, \theta') \alpha(\theta, \theta'; s) = \pi(\theta') q(\theta | \theta') p(s | \theta', \theta) \alpha(\theta', \theta; s). \quad (8)$$

This holds, for example, when the acceptance probability is

$$\begin{aligned}
\alpha(\theta, \theta'; s) &= 1 \wedge \frac{\pi(\theta')q(\theta|\theta')p(s|\theta', \theta)}{\pi(\theta)q(\theta'|\theta)p(s|\theta, \theta')} \\
&= 1 \wedge \frac{q(\theta'|\theta)p(\theta')}{q(\theta|\theta')p(\theta')} \exp \left[\sum_{i=1}^n \ell_i(\theta') - \ell_i(\theta) \right] \exp \left[\sum_{i=1}^n \Delta_i \right] \prod_{i=1}^n \left\{ \frac{\phi'_i}{\phi_i} \right\}^{s_i} \\
&= 1 \wedge \frac{q(\theta'|\theta)p(\theta')}{q(\theta|\theta')p(\theta')} \exp \left[\sum_{i=1}^n r_i(\theta, \theta'; \hat{\theta}) \right] \prod_{i=1}^n \left\{ \frac{\phi'_i}{\phi_i} \right\}^{s_i} \\
&= 1 \wedge \frac{q(\theta'|\theta)p(\theta')}{q(\theta|\theta')p(\theta)} \exp \left[\sum_{i=1}^n r_i(\theta, \theta'; \hat{\theta}) \right] \exp \left[\sum_{i=1}^n s_i \{ \log(\phi'_i) - \log(\phi_i) \} \right].
\end{aligned} \tag{9}$$

Sampling random Poisson variables S_1, \dots, S_n independently would be an $\mathcal{O}(n)$ operation that is performed at every Metropolis-Hastings iteration, and therefore not practical. To avoid such costly simulations, we use Poisson thinning (Lewis and Shedler, 1979; Bouchard-Côté et al., 2018; Bierkens et al., 2019; Cornish et al., 2019; Zhang et al., 2020) to efficiently sample the S_i at each iteration. Defining $C := \sum_{i=1}^n c_i$, we proceed as follows:

1. Sample $B \sim \text{Pois}(CM(\theta, \theta'))$.
2. Conditional on B , sample $(T_1, \dots, T_B) \sim \text{Multinomial}(B; c_1/C, \dots, c_i/C, \dots, c_n/C)$. The set $\{T_j\}_{j=1}^B$ contains the indices (possibly repeated) of data points that could be included in the likelihood evaluation.
3. For each $j \in 1, \dots, B$, include T_j in \mathcal{I} with a probability $\phi_{T_j} / \{c_{T_j} M(\theta, \theta')\}$. For each $i = 1, \dots, n$, S_i is the number of times the index i occurs in \mathcal{I} .

Marginalising Steps 1 and 2 over B , the number of times each index i appears in the set $\{T_j\}_{j=1}^B$ has a $\text{Pois}(c_i M(\theta, \theta'))$ distribution, independent of the frequencies of all other indices. Step 3 then thins down to the required distribution. Calculating C has a single $\mathcal{O}(n)$ cost at the start of the algorithm. Similarly, after an $\mathcal{O}(n)$ set up cost, Step 2 has a per-iteration cost of $\mathcal{O}(B)$ since it assigns an index to each of the B values of T_j that are non-zero. As we will see in Appendix B, B is, at most $\mathcal{O}(1)$. Lastly, Step 3 also has a per-iteration cost of $\mathcal{O}(B)$. The final set up cost of the algorithm is in finding a suitable $\hat{\theta}$, which is also $\mathcal{O}(n)$.

Algorithm 1 presents our algorithm, Metropolis-Hasting with Scalable Subsampling (MH-SS), using a delayed-acceptance (DA) formulation (Christen and Fox, 2005; Cui et al., 2011; Golightly et al., 2015; Sherlock et al., 2017; Quiroz et al., 2018b) where the MH acceptance ratio is now $\alpha(\theta, \theta'; s) = \alpha_1(\theta, \theta')\alpha_2(\theta, \theta'; s)$. In essence, this uses the approximation from the Taylor expansion about $\hat{\theta}$ to pre-screen each proposal, reducing the computational cost still further, with no additional effort. Here $\alpha(\theta, \theta'; s)$ in (9) is replaced with $\alpha_1(\theta, \theta')\alpha_2(\theta, \theta'; s)$, where

$$\alpha_1(\theta, \theta') = 1 \wedge \frac{p(\theta')q(\theta|\theta')}{p(\theta)q(\theta'|\theta)} \exp \left[\sum_{i=1}^n r_i(\theta, \theta'; \hat{\theta}) \right], \tag{10}$$

$$\alpha_{2, MHSS}(\theta, \theta') = 1 \wedge \exp \left[\sum_{i \in \mathcal{I}} s_i \{ \log(\phi'_i) - \log(\phi_i) \} \right]. \tag{11}$$

The detailed balance condition (8) is still satisfied and so the algorithm continues to target $\pi(\theta)$.

If the proposal is rejected at the pre-screening stage, then the algorithm proceeds to the next iteration and a new proposal. Though $\alpha_1(\theta, \theta')$ involves all n observations, it takes negligible

CPU time to calculate because the components in $r_i(\theta, \theta'; \hat{\theta})$ that require most of the computational effort (i.e., $\sum_{i=1}^n g_i(\hat{\theta})$ and, for second-order control variates, also $\sum_{i=1}^n H_i(\hat{\theta})$) are pre-computed before running the algorithm. This brings down the computational cost per iteration in evaluating the control variates to $\mathcal{O}(d)$ for first-order and $\mathcal{O}(d^2)$ for second-order. When the pre-screening step has been passed successfully and $\mathbb{E}(B) = CM(\theta, \theta') \geq n$, then subsampling is not used, and the remainder of a step of the (delayed-acceptance) Metropolis–Hastings is performed on the full data. Otherwise, on passing the pre-screening, the proposal θ' is accepted with probability $\alpha_{2,MHSS}(\theta, \theta'; s)$, which is calculated taking into account at most B observations, those with non-zero s_i .

Algorithm 1 Metropolis–Hastings with Scalable Subsampling (MH-SS)

```

1: Initialise:  $\theta$ .
2: for ( $t = 1$  to  $T$ ) do
3:   Sample  $\theta' \sim q(\cdot|\theta)$ .
4:   Sample  $u \sim \text{Uniform}(0, 1)$  and compute the DA-MH Stage 1 acceptance probability
    $\alpha_1(\theta, \theta')$  in (10).
5:   if  $u \leq \alpha_1(\theta, \theta')$  then
6:     if  $CM(\theta, \theta') \geq n$  then ▷ Metropolis–Hastings step on the full data
7:       Compute the DA Metropolis–Hastings Stage 2 acceptance probability:

$$\alpha_{2,MH}(\theta, \theta') = 1 \wedge \frac{p(y_{1:n}|\theta')}{p(y_{1:n}|\theta)} \exp \left[ - \sum_{i=1}^n r_i(\theta, \theta'; \hat{\theta}) \right].$$

8:       Sample  $u \sim \text{Uniform}(0, 1)$ : if  $u \leq \alpha_{2,MH}(\theta, \theta')$ , set  $\theta = \theta'$ .
9:     else ▷ Metropolis–Hastings step on subsamples
10:      Sample  $B \sim \text{Poisson}(CM(\theta, \theta'))$ 
11:       $\mathcal{I} \leftarrow \emptyset$ .
12:      for ( $b = 1$  to  $B$ ) do ▷ Subsample creation step
13:        Sample  $i_b$  such that  $P(i_b = i) = c_i/C$  for  $i = 1, \dots, n$ .
14:        Add  $i_b$  to  $\mathcal{I}$  with probability  $\frac{\phi_{i_b}(\theta)}{c_{i_b}M(\theta, \theta')}$ .
15:      end for
16:      Compute the DA MH-SS Stage 2 acceptance probability  $\alpha_{2,MHSS}(\theta, \theta')$  in (11).
17:      Sample  $u \sim \text{Uniform}(0, 1)$ : if  $u \leq \alpha_{2,MHSS}(\theta, \theta')$ , set  $\theta = \theta'$ .
18:    end if
19:  end if
20: end for
21: Output: Samples from the posterior distribution  $\pi(\theta)$ .
```

For random walk-based proposals, q , such as $\theta' \sim \mathbf{N}(\theta, V)$ for some variance matrix V , or for the Crank–Nicholson proposal with pre-conditioning based on $\hat{\pi}$ that is suggested in Cornish et al. (2019), Algorithm 1 can be applied as written. For proposals, such as that of the Metropolis-adjusted Langevin algorithm (MALA), that use $\nabla \log \pi(\theta)$, naively, the costs of proposing θ' and of evaluating both $q(\theta'|\theta)$ and $q(\theta|\theta')$ are all $\mathcal{O}(n)$. In this case a cheap, unbiased low-variance estimator of $\nabla \log \pi$ at both the proposed and current parameter values can be obtained by subsampling and using control variates; for example:

$$\widehat{\nabla} \log \pi(\theta) = \sum_{i=1}^n g_i(\hat{\theta}) + \frac{n}{m} \sum_{j=1}^m \{g_{i_j}(\theta) - g_{i_j}(\hat{\theta})\},$$

where i_1, \dots, i_m are the indices of the random subsample chosen at this iteration for estimating the gradients and $\sum_{i=1}^n g_i(\hat{\theta})$ is pre-computed.

3 Issues with existing subsampling MH algorithms

Maclaurin and Adams (2014) propose the Firefly Monte Carlo (FlyMC) algorithm, which augments the parameter space by introducing latent Bernoulli random variables. The Bernoulli success probabilities are defined so that the θ marginal of the invariant distribution of the Markov chain is exactly π . Crucially, the evaluation of the joint posterior only requires likelihood terms corresponding to the non-zero Bernoulli variables. The biggest limitation of this algorithm is the requirement of a global exponential-family lower bound that is needed on each likelihood term $B_i(\theta) \leq \ell_i(\theta)$. A secondary consideration is the trade-off between the MCMC mixing of the Bernoulli variables and the computational cost of updating them.

Similar to our proposed algorithm, scalable MH (SMH; Cornish et al., 2019) also assumes that the log-likelihood difference is bounded as in (3); however, the delayed-acceptance idea is applied repeatedly to give an overall acceptance probability of

$$\alpha_1(\theta, \theta') \prod_{i=1}^n 1 \wedge \exp(\Delta_i). \quad (12)$$

We explain the remainder of the algorithm using a formulation that is equivalent to that in Cornish et al. (2019), but using quantities more familiar from our algorithm. B and T_1, \dots, T_B are (effectively) simulated via the same mechanism as in our algorithm so that N_i , the number of repeats of the index i in the set $\{T_j\}_{j=1}^B$ has a $\text{Pois}(c_i M(\theta, \theta'))$ distribution. Then, for each i , $A_i \sim \text{Binom}(N_i, p_i)$ is created, where $p_i = -\log[1 \wedge \exp(\Delta_i)]/[c_i M(\theta, \theta')]$. Since $A_i \sim \text{Pois}(-\log[1 \wedge \exp(\Delta_i)])$, $\mathbb{P}(\sum_{i=1}^n A_i = 0)$ is exactly the product term in (12). As $(1 \wedge a)(1 \wedge b) \leq 1 \wedge ab$, the acceptance probability (12) is always lower than ours. Experiments with first-order control variates later in this section show that to avoid the acceptance rate dropping unacceptably low, the scaling parameter in the proposal $q(\theta'|\theta)$ must be reduced to well below the optimal value for the equivalent MH algorithm. Our bounds $c_i M(\theta, \theta')$ are also typically tighter than those in Cornish et al. (2019), especially in moderate to high dimensions.

The TunaMH algorithm of Zhang et al. (2020) again uses (3), but without control variates. It creates quantities ϕ_i and ϕ'_i , but with $\phi_i = [\ell_i(\theta) - \ell_i(\theta') + c_i M(\theta, \theta')]/2$. This form of ϕ_i is a special case of (5), with $\gamma = \frac{1}{2}$. Section 4.1 shows that the optimal choice of γ is always 0.

In TunaMH, where there are no control variates, $c_i M(\theta, \theta')$ is much larger (because the quantity it is bounding is much larger); however, it is also, typically, a much tighter bound on ϕ_i and ϕ'_i . As a consequence, with ϕ and ϕ' varying across the range from 0 to $c_i M(\theta, \theta')$, the acceptance ratio in (7) has a high variance and is often very low. TunaMH adds an extra term to each Poisson expectation, ϕ_i . This additional expectation lower bounds both the numerator and denominator of every term in the product in (7) and, if it is sufficiently large compared with ϕ_i and ϕ'_i , it stabilises the acceptance rate. The size of the term is *tunable* via an additional hyperparameter, giving the algorithm its name. However, this additional expectation comes at a cost of increasing $\mathbb{E}[B]$ and hence the computational cost, leading to an apparent trade-off between the acceptance rate and the subsample size.

In fact, it is a three-way trade-off. Decreasing the scaling parameter, λ , for the jumps in the MH proposal, $q(\theta'|\theta)$, decreases $\|\theta' - \theta\|$ and hence $\ell_i(\theta') - \ell_i(\theta)$ and, thus, $M(\theta, \theta')$. In this way, each ϕ_i and ϕ'_i becomes smaller compared with the additional Tuna expectation; the smaller λ helps

stabilise the acceptance probability. In reducing $\|\theta' - \theta\|$, it also reduces the computational cost via a smaller $\mathbb{E}[B]$ (the size of the final subsample) through smaller ϕ_i . The advice in Zhang et al. (2020) is to add only a small amount to each expectation so that no more than one extra observation is used on average in each subsample, and to aim for an empirical acceptance rate of around 60%. As a consequence, the Metropolis–Hastings scaling λ is reduced substantially, the Markov chain mixes more slowly and although the algorithm is more efficient than MH with *the same* λ but no subsampling, it brings no substantial improvement over an *optimally scaled* MH algorithm (which we illustrate in Figure 1).

To be more specific, consider the random-walk proposal (19) for a fixed dimension, d , and examine the effect of varying n . When the acceptance rate is reasonable, the mixing efficiency of the RWM is approximately proportional to λ^2/d , which (with d fixed) is $\mathcal{O}(\lambda^2)$, and does not depend on n . However, the computational cost of each iteration is proportional to n , giving an overall efficiency of $\mathcal{O}(\lambda^2/n)$. By contrast, for Tuna, $M(\theta, \theta') \propto \|\theta' - \theta\| = \mathcal{O}(\lambda n^{-1/2})$, by the Bernstein-von Mises Theorem, so the computational cost is $\mathcal{O}(\lambda n^{1/2})$. As with the RWM, for a reasonable acceptance rate, the mixing efficiency is proportional to λ^2 , so the overall efficiency is $\mathcal{O}(\lambda n^{-1/2})$. For the RWM, it is possible to choose $\lambda = \mathcal{O}(1)$ and maintain a good acceptance rate; in contrast, in practice for Tuna (see, for example, Table 7), to follow the advice in Zhang et al. (2020) and keep the acceptance rate around 60%, we find that λ must be decreased in proportion to $n^{-1/2}$, leading to the same order of efficiency as the RWM; i.e., there is no free lunch.

Figure 1 shows the effective sample size (ESS) per second, average batch sizes and acceptance rates as dimension d increases for a logistic regression model with $n = 30,000$ observations. It compares three algorithms: the RWM and versions of the same algorithm using TunaMH and SMH with first-order control variates, which we refer to as SMH-1. Panel (b) shows that Tuna uses a fraction of the observations that the full-batch RWM uses, but it is clear from Panel (a) that TunaMH is not substantially more efficient than the RWM, especially as d increases. For example, for $d = 5$ and $d = 60$, Tuna requires on average per MCMC iteration subsamples of sizes $10^{1.38} \approx 24$ and $10^{2.47} \approx 301$, respectively. As recommended in Zhang et al. (2020), we set the Tuna parameter so that the expected number of additional data points was typically just below 1 and tuned the scaling parameter of the proposal distribution to return an acceptance rate of 60%, as shown in panel (c). The fact that TunaMH uses a fraction of n makes it significantly faster than the RWM, but it does not make it substantially more efficient because of the small scaling parameter of the proposal distribution that is needed to achieve the target acceptance rate.

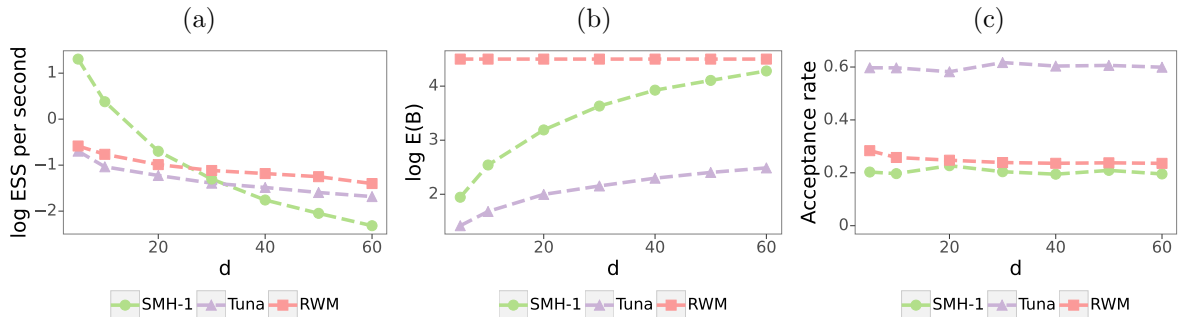


Figure 1: Acceptance rates and ESS per second for SMH-1, Tuna and RWM. The results are based on synthetic datasets generated from a logistic regression model with $n = 10^{4.5} \approx 30,000$ observations. The y-axis of panels (a) and (b) are presented in the logarithm base 10.

All of the algorithms in Figure 1 use $q(\theta'|\theta) = \text{N}(\theta, \frac{\lambda^2}{d}V_d)$ as the proposal distribution, where $V_d = -[H(\hat{\theta})]^{-1}$ denotes minus the inverse of the Hessian at an estimate $\hat{\theta}$ near the mode and $\lambda > 0$ is a scaling parameter that requires tuning. Following the literature on optimal scaling for the random-walk Metropolis algorithm (Gelman et al., 1997; Roberts and Rosenthal, 2001; Sherlock and Roberts, 2009), we set $\lambda = 2.38$. This choice leads, in the limit as $d \rightarrow \infty$, to an acceptance rate of approximately 23.4%, as shown in panel (c) of Figure 1. In sharp contrast, for Tuna, λ is set from 0.03 ($d = 5$) to 0.1 ($d = 60$) to maintain an acceptance rate of around 60%; see Table 6 in Appendix C.3 for all values.

The bounds on the log-likelihood differences used in the SMH algorithm are quite loose (see Section 5), even for moderate d , especially when using first-order control variates. In practice, looser bounds imply that larger subsamples need to be evaluated in the MH ratio, leading to increased computational time and lower efficiency. Panel (a) of Figure 1 shows that SMH-1's ESS per second deteriorates more quickly with dimension than that of Tuna and the RWM. The explanation for this is two-fold. Firstly, Panel (b) shows the steady increase in SMH's average batch size as the number of variables in the linear predictor of the logistic regression model increases. The greater the batch size, the slower the algorithm. For example, for $d = 5$ and $d = 50$, SMH's average batch size jumps from $10^{1.94} \approx 88$ to $10^{4.10} \approx 12,751$. For $d = 60$, almost all n observations are required. Consequently, in order to keep a constant acceptance rate at which SMH-1 is most efficient as dimension d changes, it is necessary to reduce the scaling parameter in the proposal distribution. For the results presented in Figure 1, λ varied from 2 ($d = 5$) to 0.65 ($d = 60$).

In Sections 5 and 6, we empirically show through simulation experiments and applications to real-world datasets that our proposed method, MH-SS, is substantially more efficient than Tuna and the RWM and that it requires substantially fewer observations than SMH for both first- and second-order control variates. The improvements over TunaMH are a direct consequence of the use of control variates with a good bound on $M(\theta, \theta')$ and of the optimal choice of γ . The improvement over SMH is due to the control variate bound being tighter and scaling better with dimension than that in SMH and because the MH-SS acceptance probability is a product of two terms, rather than of many terms, all bounded above by 1. Our tighter bounds on the log-likelihood differences are introduced in Section 4.2. As we will show in Section 4.1, the optimal choice of γ in (5) leads to larger acceptance rates, which helps maximise the computational efficiency of our algorithms. In addition, in Appendix B (see also Section 4.3), through an asymptotic analysis, we compare our proposed bounds with those of SMH and show that our bounds are at least a factor of $d^{1/2}$ tighter. Finally, Section 4.4 studies both the scaling and acceptance rate that maximise the efficiency for our proposed methods in the case of a RWM proposal. In contrast to the standard RWM algorithm, our results suggest that the optimal acceptance rate for the MH-SS algorithm is approximately 45%.

4 Theoretical results

We now present theoretical results to support our proposed method. First, we demonstrate that the acceptance rate of MH-SS is maximised when γ is set to zero in (5). Then, we present general bounds for the log-likelihood differences considering first- and second-order control variates. The proofs of all theoretical results in this section are deferred to Appendix A.

4.1 Optimality with respect to ϕ

Theorem 1. Let $\alpha_2^{(\gamma)}(\theta, \theta')$ be the acceptance probability $\alpha_{2, \text{MHSS}}(\theta, \theta')$ from (11) when ϕ_i and ϕ'_i are defined as in (5) and (6). Then for any fixed θ and θ' , $\alpha_2^{(\gamma)}(\theta, \theta')$ is a decreasing function of γ , so is maximised when $\gamma = 0$.

Proof: See Section A.1 in the Appendix. \square

Since $\alpha_1(\theta, \theta')$ in (10) does not depend on γ , this implies that the overall acceptance probability is maximised when $\gamma = 0$. Furthermore, the number of samples used in the calculation depends only on the bounds $c_i M(\theta, \theta')$ and so the computational cost is not affected by γ . Since the proposal, $q(\theta'|\theta)$, is the same, whatever the value of γ , Peskun (1973) and Tierney (1998) lead to the following result:

Corollary 1. The efficiency of Algorithm 1 in terms of effective samples per second is maximised when $\gamma = 0$.

To illustrate the practical implications of Theorem 1, we perform simulation experiments using our method with first-order control variates on a logistic regression model. For each combination of $n = (10^3, 10^4, 10^5)$ and $d = (5, 10, 30, 50, 100)$, we set γ to 0, 0.5 and 1. Setting $\gamma = 0.5$ corresponds to employing the ϕ function in (5) used by Zhang et al. (2020) (albeit with control variates and without the additional Tuna term), thereby illustrating the acceptance rate of our method if we were to use this sub-optimal choice of γ . Figure 2 presents acceptance rates of our proposed method with first-order control variates obtained from 10 Monte Carlo simulations. Unsurprisingly, the acceptance rates of MH-SS are maximised when $\gamma = 0$, regardless of the values of n and d , which is consistent with Theorem 1. Conversely, $\gamma = 0.5$ consistently yields lower acceptance rates compared to $\gamma = 0$, while $\gamma = 1$ exhibits the poorest results. Since the algorithms differ only in terms of the value of γ , Corollary 1 states that the one with the highest acceptance rate inevitably exhibits the largest effective sample size. We also investigated the effect of γ on acceptance rates of our method with second-order control variates. Whilst the same ordering with γ was evident, the differences were less pronounced, and we omit them for the sake of conciseness.

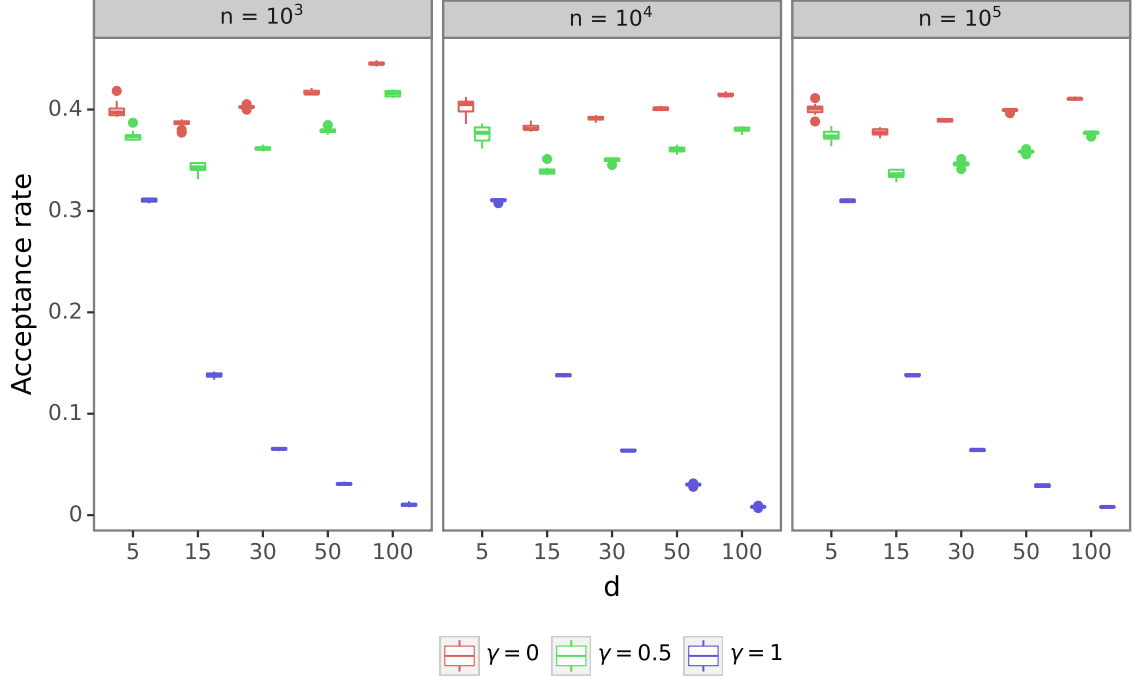


Figure 2: Acceptance rates of the proposed method with first-order control variates. For each combination of γ , n and d , 10 synthetic datasets are generated from a logistic regression model.

4.2 Bounds on the remainder terms

Our method assumes that $|\ell_i(\theta') - \ell_i(\theta) - r_i^{(k)}(\theta, \theta')| \leq c_i^{(k)} M^{(k)}(\theta, \theta')$, for $k = 1, 2$. Bounds on these differences are provided in Cornish et al. (2019); however, these bounds are loose as dimension d increases. In this section, we provide tighter generic bounds and then refine these further in the case of regression models.

4.2.1 General bounds on the remainders

We first prove general bounds which will be useful in all of our examples in Sections 5 and 6 and many others besides. These general bounds then lead to specific forms in each example; see the end of this subsection for cases of logistic regression, probit regression and a form of Poisson regression.

Theorem 2. Let $\theta, \theta', \hat{\theta} \in \mathcal{X} \subseteq \mathbb{R}^d$ and let \mathcal{A} be the triangle with vertices at $\theta, \theta', \hat{\theta}$. Let $\ell: \mathbb{R}^d \rightarrow \mathbb{R}$ and let $g(\theta) = \nabla \log \pi(\theta)$ and $H(\theta) = \nabla \nabla^\top \log \pi(\theta)$. Let $\|v\|$ indicate the L_2 norm of v . Set

$$r^{(1)}(\theta, \theta'; \hat{\theta}) := (\theta' - \theta)^\top g(\hat{\theta}), \quad (13)$$

$$r^{(2)}(\theta, \theta'; \hat{\theta}) := (\theta' - \theta)^\top g(\hat{\theta}) + (\theta' - \theta)^\top H(\hat{\theta}) \left\{ \frac{1}{2}(\theta' + \theta) - \hat{\theta} \right\}. \quad (14)$$

- Suppose that there exists $x \in \mathbb{R}^d$ and $M_1 \geq 0$ such that for any $\theta_1 \in \mathcal{A}$ and $u, v \in \mathbb{R}^d$,

$$|u^\top H(\theta_1)v| \leq |x^\top u| |x^\top v| M_1. \quad (15)$$

Then

$$\left| \ell(\theta') - \ell(\theta) - r^{(1)}(\theta, \theta'; \hat{\theta}) \right| \leq |x^\top(\theta' - \theta)| \max \left(|x^\top(\theta - \hat{\theta})|, |x^\top(\theta' - \hat{\theta})| \right) M_1. \quad (16)$$

If, instead, for any $\theta_1 \in \mathcal{A}$ and $u, v \in \mathbb{R}^d$, there exists $M_2 \geq 0$ such that

$$|u^\top H(\theta_1)v| \leq \|u\| \|v\| M_2$$

then

$$\left| \ell(\theta') - \ell(\theta) - r^{(1)}(\theta, \theta'; \hat{\theta}) \right| \leq \|\theta' - \theta\| \max \left(\|\theta - \hat{\theta}\|, \|\theta' - \hat{\theta}\| \right) M_2.$$

- Alternatively, suppose that there exists $x \in \mathbb{R}^d$ and $L_1 \geq 0$ such that for any $\theta_1, \theta_2 \in \mathcal{A}$ and $u, v \in \mathbb{R}^d$

$$\left| u^\top \{H(\theta_2) - H(\theta_1)\} v \right| \leq |x^\top u| |x^\top v| |x^\top(\theta_2 - \theta_1)| L_1. \quad (17)$$

Then

$$\begin{aligned} \left| \ell(\theta') - \ell(\theta) - r^{(2)}(\theta, \theta'; \hat{\theta}) \right| &\leq \frac{1}{12} |x^\top(\theta' - \theta)|^3 L_1 \\ &\quad + \frac{1}{2} |x^\top(\theta' - \theta)| |x^\top(\theta - \hat{\theta})|^2 L_1 \\ &\quad + \frac{1}{2} |x^\top(\theta' - \theta)| |x^\top(\theta' - \hat{\theta})|^2 L_1. \end{aligned} \quad (18)$$

If, instead, for any $\theta_1, \theta_2 \in \mathcal{A}$ and $u, v \in \mathbb{R}^d$, there exists $L_2 \geq 0$ such that

$$\left| u^\top \{H(\theta_2) - H(\theta_1)\} v \right| \leq \|u\| \|v\| \|\theta_2 - \theta_1\| L_2,$$

then

$$\left| \ell(\theta') - \ell(\theta) - r^{(2)}(\theta, \theta'; \hat{\theta}) \right| \leq \frac{1}{12} \|\theta' - \theta\|^3 L_2 + \frac{1}{2} \|\theta' - \theta\| \|\theta - \hat{\theta}\|^2 L_2 + \frac{1}{2} \|\theta' - \theta\| \|\theta' - \hat{\theta}\|^2 L_2.$$

Proof: See Section A.2 in the Appendix. \square

Remark 1. Let κ be the magnitude of the largest eigenvalue of a symmetric matrix W , where $W = H(\theta_1)$ or $W = H(\theta_2) - H(\theta_1)$. In general, $a^\top W b \leq \kappa \|a\| \|b\|$, motivating the two unnumbered conditions. In the special case of a single observation from a generalised linear model, however, it will turn out that we may obtain a more subtle bound by taking x to be a covariate vector and using the forms in (16) and (18).

4.2.2 Regression models: Further improvement on bounds

We now specialise to the case where each observation is a realisation from a regression model with a covariate vector, x , regression coefficients, β , and observation, y , such that the likelihood for the observation is $\ell(\beta) = \mathfrak{h}(\eta; y)$, where $\eta = x^\top \beta$.

In the following, we abbreviate $\mathfrak{h}(\eta; y)$ to $\mathfrak{h}(\eta)$. Firstly,

$$g(\beta) = \nabla_\beta \ell = (\nabla_\beta \eta) \mathfrak{h}'(\eta) = x \mathfrak{h}(\eta) \quad \text{and} \quad H(\beta) = \nabla_\beta \nabla_\beta^\top \ell = x x^\top \mathfrak{h}''(\eta).$$

Thus, $|a^\top H(\beta)b| = |x^\top a| |x^\top b| |\mathfrak{h}''(\eta)|$; also, with $\eta_1 = x^\top \beta_1$ and $\eta_2 = x^\top \beta_2$,

$$\begin{aligned} |a^\top \{H(\beta_2) - H(\beta_1)\}b| &= |a^\top x \{\mathfrak{h}''(\eta_2) - \mathfrak{h}''(\eta_1)\}x^\top b| = |x^\top a| |x^\top b| |\eta_2 - \eta_1| |\mathfrak{h}'''(\eta_*)| \\ &= |x^\top a| |x^\top b| |x^\top (\beta_2 - \beta_1)| |\mathfrak{h}'''(\eta_*)|, \end{aligned}$$

for some $\eta_* \in [\eta_1, \eta_2]$. So we can find appropriate bounds for (15) and (17) by bounding $|\mathfrak{h}''(\eta; y)|$ and $|\mathfrak{h}'''(\eta; y)|$.

Before doing this, however, we tighten our general bounds further in the case of a regression model, improving over the obvious bound that arises from repeated application of the Cauchy-Schwarz inequality. The improvement helps in practice because in high-dimensions, “most” vectors are almost perpendicular to each other so the inner product ω that we will define is often close to 0.

Lemma 1. *Let $u, v, x \in \mathbb{R}^d$ and let $\omega := u \cdot v / (\|u\| \|v\|)$, then for $k > 0$, $|u \cdot x|^k |v \cdot x| \leq D_k(\omega) \|u\|^k \|v\| \|x\|^{k+1}$, where*

$$D_k(\omega) = \frac{1}{c_k(\omega)(k+1)^{(k+1)/2}} \{k + |\omega| c_k(\omega)\}^{(k+1)/2},$$

$$\text{and } c_k(\omega) = \sqrt{k + \frac{1}{4}(k-1)^2 \omega^2} - \frac{1}{2}(k-1)|\omega|.$$

Proof: See Section A.3 in the Appendix. \square

Remark 2. *We make three points.*

1. *When $k = 1$ and $c_k = 1$, $D_k(\omega)$ simplifies to $D_1(\omega) = \{1 + |\omega|\}/2$. Giving a typical improvement of nearly a factor of 2 over the obvious application of the Cauchy-Schwarz inequality.*
2. *When u and v are aligned, then $\omega = 1$ and $c_k = 1$ implies $D_k(\omega) = 1$, which retrieves the bound from the Cauchy-Schwarz inequality.*
3. *When u and v are orthogonal, as is usually approximately the case in high dimensions, $\omega = 0$, $c_k = \sqrt{k}$ and*

$$D_k = \frac{1}{\sqrt{k}} \left(1 - \frac{1}{k+1}\right)^{(k+1)/2} \uparrow \frac{1}{\sqrt{k}} \exp(-1/2).$$

So in typical high-dimensional cases, we gain a factor of $e^{-1/2}/\sqrt{k}$ over the Cauchy-Schwarz inequality.

Combining Lemma 1 with Theorem 2 then gives the following, which we apply in practice for each of our regression models.

Corollary 2. *Consider a likelihood term $\ell(\theta) = \mathfrak{h}(x^\top \theta; y)$ and define*

$$\omega := \frac{(\theta - \hat{\theta}) \cdot (\theta' - \theta)}{\|\theta - \hat{\theta}\| \|\theta' - \theta\|} \quad \text{and} \quad \omega' := \frac{(\theta' - \hat{\theta}) \cdot (\theta' - \theta)}{\|\theta' - \hat{\theta}\| \|\theta' - \theta\|}.$$

If $\|\mathfrak{h}''(x^\top \theta; y)\| \leq M(y)$ then,

$$\left| \ell(\theta') - \ell(\theta) - r^{(1)}(\theta, \theta'; \hat{\theta}) \right| \leq \|x\|^2 \|\theta' - \theta\| \max \left[\|\theta - \hat{\theta}\| D_1(\omega), \|\theta' - \hat{\theta}\| D_1(\omega') \right] M(y).$$

Alternatively, if $\|\mathfrak{h}'''(\theta; y)\| \leq L(y)$ then

$$\left| \ell(\theta') - \ell(\theta) - r^{(2)}(\theta, \theta'; \hat{\theta}) \right| \leq \frac{\|x\|^3 \|\theta' - \theta\|}{2} \left\{ \frac{1}{6} \|\theta' - \theta\|^2 + \|\theta - \hat{\theta}\|^2 D_2(\omega) + \|\theta' - \hat{\theta}\|^2 D_2(\omega') \right\} L(y).$$

In moderate to high dimensions, most of the time, $\theta' - \theta$ is close to perpendicular to both $\theta - \hat{\theta}$ and $\theta' - \hat{\theta}$, so Corollary 2 gives a reduction of (typically) close to a factor of 2 for the first-order bound and around 2.5 for the second-order bound. In moderate to high dimensions, most x are also close to perpendicular to the three vectors of interest, so the true remainder is typically much smaller than even this tighter bound.

For the regression models in Sections 5 and 6, we use the following values (justified in Section A.4):

- Logistic regression: $M(y) = 1/4$ and $L(y) = \sqrt{3}/18$;
- Probit regression: $M(y) = 1$ and $L(y) = 0.3$;
- Poisson regression with an expectation of $\log[1 + \lambda \exp(\eta)]$ for any fixed λ : $M(y) = 0.25 + 0.168y$ and $L(y) = \sqrt{3}/18 + 0.061y$.

For the Tuna algorithm with logistic regression, we may use the bound $|\ell_i(\theta') - \ell_i(\theta)| \leq \|x_i\| \|\theta' - \theta\|$ (e.g., Cornish et al., 2019; Zhang et al., 2020). For Poisson regression with an expectation of $\log[1 + \exp(\eta)]$, the bound is $|\ell_i(\theta') - \ell_i(\theta)| \leq \|x_i\| \max(1, y_i) \|\theta' - \theta\|$.

4.3 Computational Cost

In Appendix B, we consider a sequence of posterior distributions in the multivariate-normal Bernstein-von Mises limit and examine the random walk Metropolis proposal using a suitable scaling and variance matrix. We show that the computational cost per iteration of MH-SS is $\Theta(d^{3/2})$ when using $r_i^{(1)}$ and $\Theta(d^3/n^{1/2})$ when using $r_i^{(2)}$. We also show that whichever control variate is used, the corresponding costs when using the bounds in Cornish et al. (2019) are at least a factor of $d^{1/2}$ larger.

4.4 Tuning the MH-SS proposal

In this section, we provide guidelines for the choice of the scaling parameter λ in the special case of a random-walk Metropolis proposal:

$$\theta' \sim \mathbf{N} \left(\theta, \frac{\lambda^2}{d} V_d \right), \quad (19)$$

where d is the dimension of θ and V_d is a d -dimensional positive definite matrix. In our analysis, we set $V_d = -[H(\hat{\theta})]^{-1}$, where $[H(\hat{\theta})]^{-1}$ represents the inverse of the Hessian at an estimate $\hat{\theta}$ near the mode. In the large- n Bernstein-von Mises limit, this is equivalent to exploring a d -dimensional standard Gaussian posterior for $\psi = \sqrt{V_d}^{-1} \theta$, with a proposal of $\psi' \sim \mathbf{N}(\psi, (\lambda^2/d) I_d)$ and, as such, fits squarely within the framework of previous analyses of the high-dimensional limit (Gelman et al., 1997; Roberts and Rosenthal, 2001; Sherlock and Roberts, 2009; Sherlock et al., 2021).

Sherlock et al. (2021) investigate the tuning of delayed-acceptance random walk Metropolis algorithms. However, while the MH-SS algorithms do have a delayed-acceptance component,

they have two specific properties that, respectively aid and necessitate a new treatment: the extreme accuracy/inaccuracy of the approximate target and an approximately linear relationship between the proposal scaling and the computational cost.

The computational cost per iteration is approximately proportional to the number of data points used and the expectation of this is proportional to $M(\theta, \theta')$. With the proposal (19), $\|\psi' - \psi\|_2 = \Theta(1)$, whereas both $\|\psi - \hat{\psi}\|_2$ and $\|\psi' - \hat{\psi}\|_2$ are $\Theta(d^{1/2})$, where $\hat{\psi} = \sqrt{V_d}^{-1}\hat{\theta}$. Provided V_d is well-conditioned, $\|\theta' - \theta\|_2$ is, therefore, also a factor of $d^{1/2}$ smaller than either $\|\theta - \hat{\theta}\|_2$ or $\|\theta' - \hat{\theta}\|_2$; see also the analysis in Appendix B. Theorem 2 then shows that for both first- and second-order control variates, $M(\theta, \theta') \propto \lambda$. This justifies the more formal:

Assumption 1. *The computational cost per iteration of both MH-SS-1 and MH-SS-2 is proportional to λ .*

In Appendix D, we argue for the following assumption, which we have observed in all of our empirical studies (see, for example, Figure 3):

Assumption 2. *For first-order control variates, $\mathbb{E}[\alpha_1(\theta, \theta')] \approx 1$ and for values of θ' that pass the screening stage, $\mathbb{E}[\alpha_{2, \text{MHSS}}(\theta, \theta')] \approx \mathbb{E}[\alpha_{\text{RWM}}(\theta, \theta')]$. For second-order control variates, $\mathbb{E}[\alpha_1(\theta, \theta')] \approx \mathbb{E}[\alpha_{\text{RWM}}(\theta, \theta')]$ and for values of θ' that pass the screening stage, $\mathbb{E}[\alpha_{2, \text{MHSS}}(\theta, \theta')] \approx 1$.*

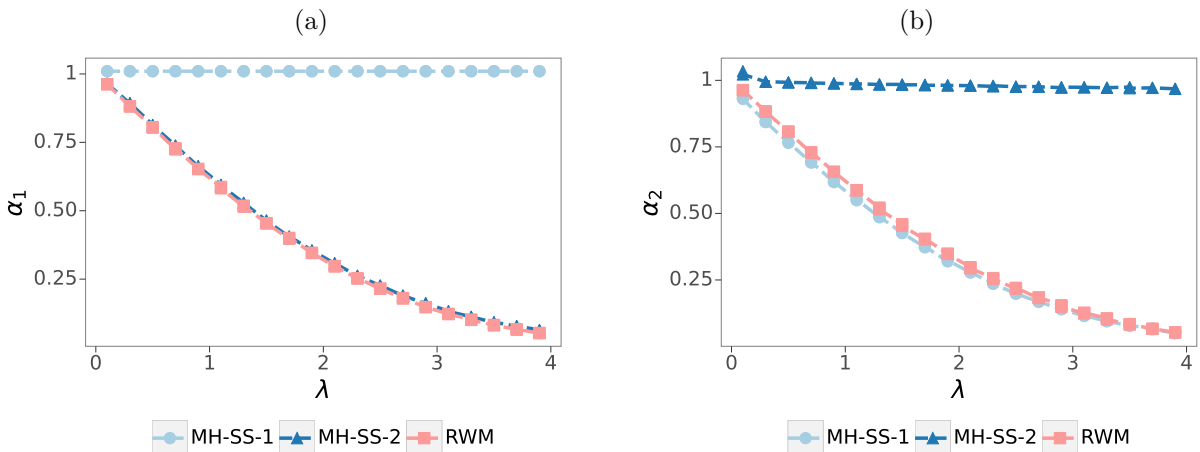


Figure 3: Acceptance rates: α_1 in (10) on the left and α_2 in (11) on the right for a logistic regression target in dimension $d = 100$ with $n = 30,000$ observations, and with covariates and true coefficients simulated as described in Section 5.

Thus, whichever form of control variate is used, we anticipate that the expected acceptance rate for a given scaling will be approximately the same as the expected acceptance rate for the RWM algorithm with that scaling. High-dimensional asymptotics for the Metropolis–Hastings algorithm with a RWM proposal (19) (e.g., Gelman et al., 1997; Roberts and Rosenthal, 2001; Sherlock and Roberts, 2009) provide a limiting expected acceptance rate of $2\Phi(-J\lambda/2)$ for some constant, J , that depends on the roughness of the posterior; with our choice of V_d , $J = 1$. The expected squared jumping distance of the i th component of θ is

$$\text{ESJD}(\lambda) = \mathbb{E} \left[\left(\theta_i^{(j)} - \theta_i^{(j+1)} \right)^2 \right],$$

where $\theta^{(j)} \sim \pi$ is the j th value in the MCMC chain and $\theta^{(j+1)}$ is the $j + 1$ th. This is a natural measure of the efficiency of the algorithm and, in the case of a limiting diffusion, is exactly

the right measure of the efficiency in the high-dimensional limit as it is proportional to the speed of the limiting diffusion. In this limit, the ESJD is proportional to the product of the expected acceptance probability and the square of the scaling parameter, $\text{ESJD} \propto 2\lambda^2\Phi(-\lambda/2)$. Maximising this quantity leads to the well-known optimal acceptance rate of 0.234 of the RWM algorithm.

Given Assumption 1, however, the overall efficiency for MH-SS algorithms is proportional to

$$\frac{\text{ESJD}(\lambda)}{\lambda} \propto 2\lambda\Phi(-\lambda/2).$$

This is maximised at $\lambda_{opt} \approx 1.50$ which gives an acceptance rate of $2\Phi(-\lambda_{opt}/2) \approx 0.452$.

We found this advice to hold true in all of our empirical studies, an example of which is given in Figure 4.

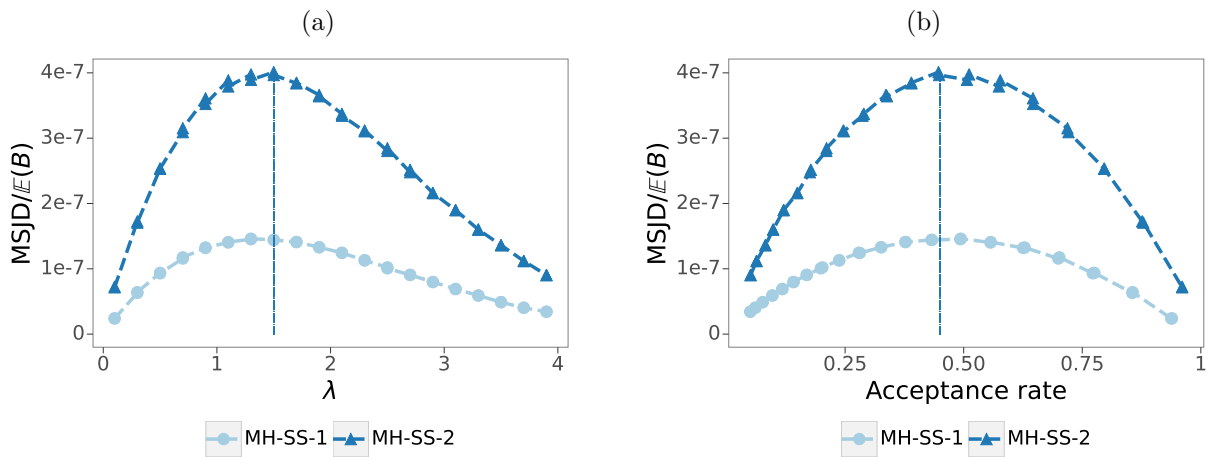


Figure 4: Optimal scaling for the MH-SS algorithms based on synthetic data from a logistic regression model with $n = 30,000$ observations and $d = 100$ covariate parameters, including an intercept. The efficiency metric ($\text{MSJD}/\mathbb{E}(B)$) is plotted as function of (a) the scaling parameter (λ) and (b) the empirical acceptance rate.

The same argument applies to any algorithm that uses our control variates, provided that for any reasonable scaling, λ , the overall acceptance rate is close to that for the RWM. The SMH bounds used in Cornish et al. (2019) are reproduced in Appendix B.2 and have only a weak relative dependence on λ . Consequently, we might expect SMH-2 to be optimally scaled when the acceptance rate is around 0.234. Figure 10 in Appendix C verifies both of these points for a particular logistic regression scenario. It also shows that the behaviour of the SMH-1 acceptance rate on λ is very different to that of the RWM. We find that the scaling must decrease more quickly with dimension than λ/\sqrt{d} to maintain a reasonable acceptance rate as dimension increases. Although there is no obviously optimal acceptance rate that we might expect to hold across different scenarios, we observed empirically through simulation experiments with various numbers of observations n (from 30,000 to 100,000) and dimensions d (from 10 to 100) that the optimal scaling parameter for SMH-1 is in the range between 0.5 to 1.5. Furthermore, for each combination of n and d , a scaling of $\lambda = 1$ achieved at least 80% of the optimal efficiency for that combination. Consequently, in Sections 5 (simulation experiments) and 6 (real-world applications), we set $\lambda = 1$ for SMH-1.

5 Simulation experiments

In this section, we compare the MH-SS algorithm against the Tuna, SMH and MH algorithms, all using random-walk proposals. We apply them to a logistic regression model and a form of the Poisson regression model. For MH-SS and SMH, we consider first- and second-order control variates, which we denote by MH-SS-1 and MH-SS-2; with the same convention for SMH. We obtain an estimate of the posterior mode $\hat{\theta}$ through the stochastic gradient descent algorithm (Robbins and Monro, 1951). The Tuna algorithm increases $\mathbb{E}[B]$ by $\chi C^2 M(\theta, \theta')^2$, where χ is the additional tuning parameter. We follow the heuristic proposed by Zhang et al. (2020), choosing χ so as to increase the expected number of simulations by less than 1 across most combinations of (θ, θ') . To aid reproducibility, we record the value of the Tuna tuning parameter, χ , used each time in Table 7 in Appendix C.3. For all methods, the proposal distribution is of the form (19) with V_d set to $-[H(\hat{\theta})]^{-1}$, where $H(\hat{\theta})$ denotes the Hessian at our approximation to the posterior mode and $\lambda > 0$ is a scaling parameter. For each method, λ was chosen based on the maximisation of the mean squared jump distance (MSJD) divided by the average subsample size, $\mathbb{E}(B)$. Following Section 4.4, we set $\lambda = 1.5$ for MH-SS-1 and MH-SS-2, $\lambda = 1$ for SMH-1, $\lambda = 2$ for SMH-2 and $\lambda = 2.38$ for the RWM. In all simulation experiments carried out in this section, the ESSs are at least 200 for all algorithms. To ensure the computational times are comparable, we implemented all methods in Python 3.9.6 (Van Rossum and Drake, 2009).

5.1 Logistic regression

To empirically demonstrate the benefits of the proposed method, we initially test it on synthetic datasets generated from a succession of logistic regression models with varying data size, n , and parameter size, d . We sample each covariate (except the intercept) independently as $x_{i,j} \sim \mathcal{N}(0, 1/d)$ and simulate independent $\beta_j \sim \mathcal{N}(0, 1)$. These choices ensure the linear predictor, $x_i^\top \beta$, remains $\mathcal{O}(1)$ as d increases and the probabilities obtained from the logistic function applied to the linear predictor are well distributed around 0.5.

For each combination of n and d , we run once each of the 6 algorithms under consideration and calculate the effective sample size (ESS; Green and Han, 1992; Liu and Chen, 1995) per second as a metric of efficiency. Additionally, we examine other metrics such as the average expected batch size, which we denote $\mathbb{E}(B)$; Appendix C presents the results in terms of the alternative efficiency metric of ESS divided by $\mathbb{E}(B)$. To highlight any power-law relationships and enable all algorithms to be jointly displayed, results involving the number of observations, n , average expected batch size, $\mathbb{E}(B)$, and ESS per second are presented on a logarithmic scale.

Figure 5 shows how the average batch size varies by n and d . As argued in Appendix B, the algorithms based on the second-order control variates use fewer data values than their first-order counterparts and require even fewer as n increases. Since the bounds we propose are tighter than those of SMH, the MH-SS algorithm uses less data. When $d = 10$, SMH-2 sometimes uses fewer observations than MH-SS-1, but MH-SS-2 always uses the fewest; in all other dimensions considered, the MH-SS algorithms used fewer observations than the SMH algorithms. For example, when $d = 50$ and $n < 10^4$, SMH requires all n observations, whereas MH-SS requires fewer than n observations, even for $n = 10^3$. In all scenarios, Tuna and MH-SS-1 require a similar subsample size, the only exception being $d = 100$ where Tuna uses fewer observations.

Figure 6 compares the ESS per second across all methods. As expected, the ESS per second of MH-SS with first- and second-order control variates is greater than that of either SMH algorithm, except when $d = 10$, where SMH-2 outperforms MH-SS-1. For $d = 10$, MH-SS-2 and SMH-2 exhibit similar efficiency for $n = 10^5 = 100,000$, even though the former uses fewer

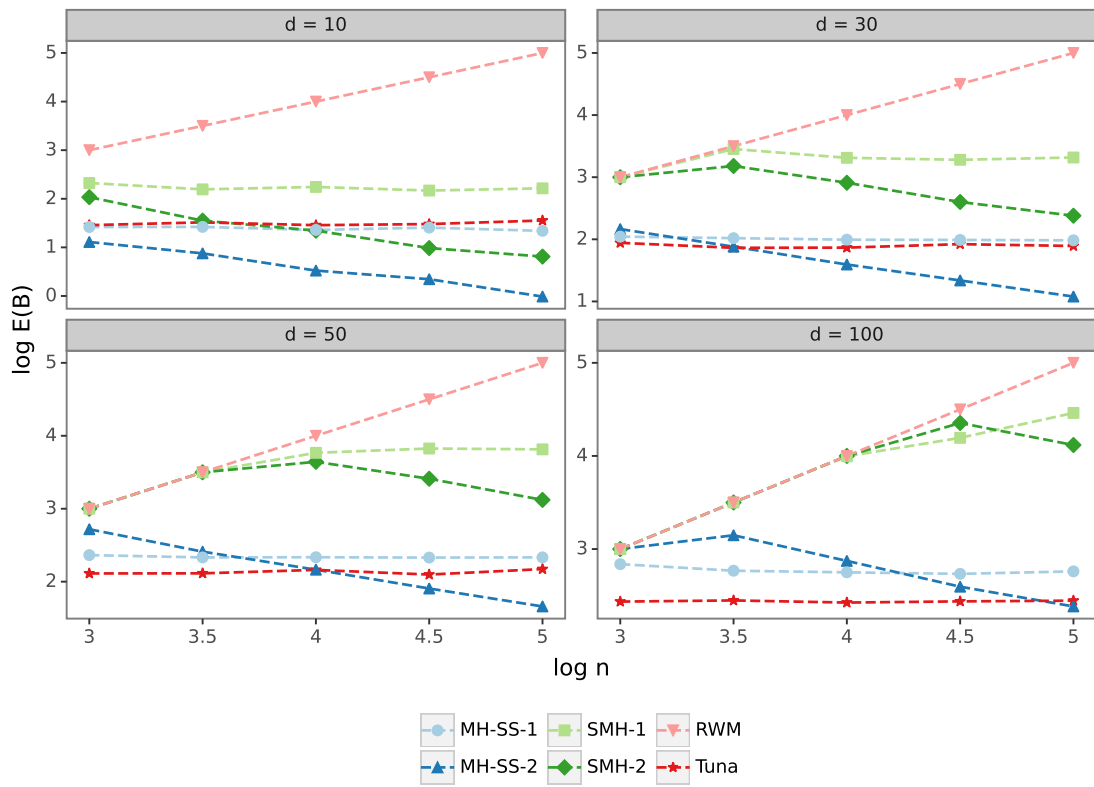


Figure 5: Average batch size for MH-SS, SMH and RWM for the logistic regression model. For RWM, the average batch size is n . Both axes are presented in the logarithm base 10.

observations. To understand this, we recall the results in the left-hand upper panel of Figure 5, where it is possible to see that $\mathbb{E}(B) \approx 10^0 = 1$ for MH-SS-2, while $\mathbb{E}(B) \approx 10^1 = 10$ for SMH-2. In practice, we observe that the run-time differences are tiny in cases where the average batch sizes are small, helping to explain the similarity in terms of efficiency. However, as d increases, the efficiency gap becomes more pronounced because the SMH bounds are at least a factor of $d^{1/2}$ worse than the equivalent MH-SS bound. Even for $d = 30$, SMH-2 would be a competitive option against RWM only for $n > 10^{3.5}$, while SMH-1 demonstrates relatively poor performance for all considered dimensions.

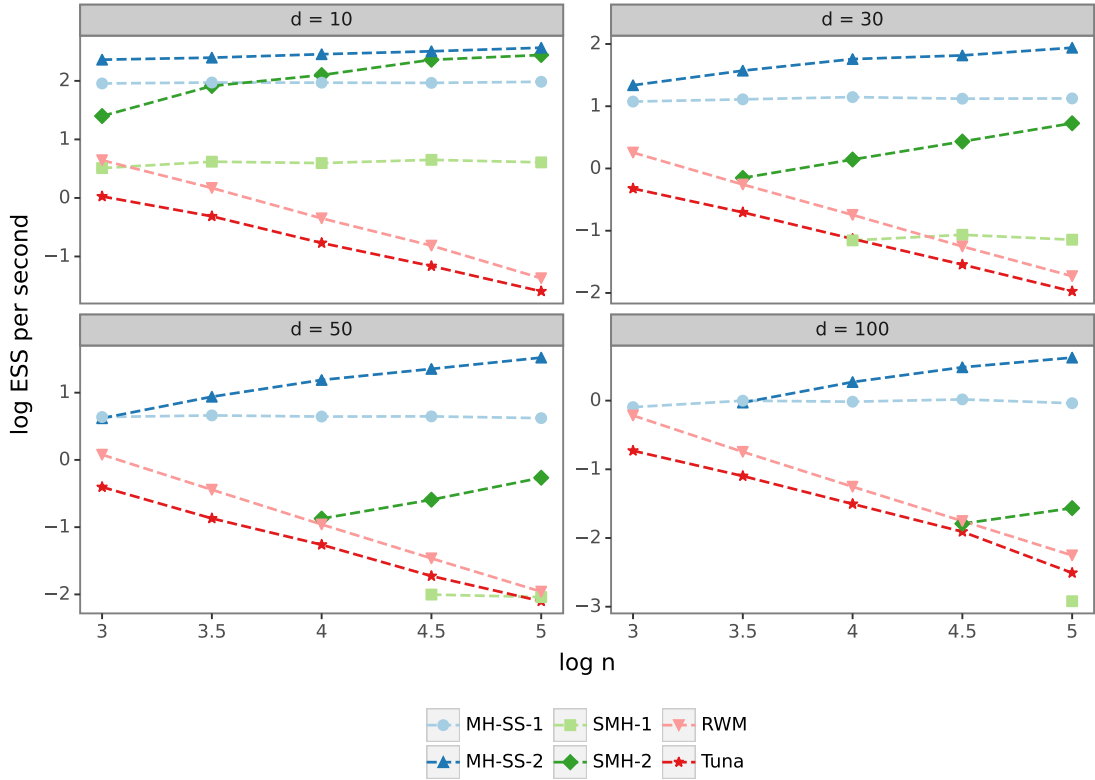


Figure 6: ESS per second of MH-SS, SMH and RWM for the logistic regression model. Both axes are presented in the logarithm base 10. Some ESSs are omitted because $\mathbb{E}(B) \geq n$, which implies the use and efficiency of the RWM algorithm.

Though Tuna and MH-SS-1 require a similar subsample size for all scenarios considered in Figure 5, except for $d = 100$, MH-SS with first- and second-order control variates outperform Tuna in all dimensions in terms of efficiency. As stated in Section 3, Tuna tends to favour smaller subsample sizes in detriment of computational efficiency and, as argued in Section 3, its performance is comparable to the RWM algorithm. To recap, the heuristic proposed by Zhang et al. (2020) aims for an acceptance rate of 60% and minimises the impact of the Tuna tuning parameter on the average batch size. As result, in practice Tuna takes tiny steps when exploring the posterior distribution. This means it uses small subsample sizes and thus has low per-iteration run-time; however, such an approach is inefficient from the effective sample size viewpoint as small step sizes lead to high auto-correlation in the Markov chain.

5.2 Decomposing the improvements over SMH

Tuna uses no more information than the RWM, so it is unsurprising that their efficiencies are similar and that MH-SS’s careful use of control variates leads to a substantial increase in efficiency. We now investigate the algorithms that use control variates, and separate the drivers of the superior performance of MH-SS over SMH.

Both SMH and our proposed method bound $|\ell_i(\theta') - \ell_i(\theta) - r_i^{(k)}(\theta, \theta'; \hat{\theta})| \leq c_i^{(k)} M^{(k)}(\theta, \theta')$, for $k = 1, 2$, though with different $c_i^{(k)}$ and $M^{(k)}(\theta, \theta')$, so we created a hybrid algorithm named SMH-NB. This hybrid approach combines the structure of SMH, which is detailed in Algorithm 1 of [Cornish et al. \(2019\)](#), with our bounds, $c_i^{(k)}$ and $M^{(k)}(\theta, \theta')$, from Section 4.2.2. We compare these hybrid algorithms with the vanilla SMH and MH-SS to separate the benefit brought by these bounds from the other benefits of MH-SS. Unlike the vanilla SMH, the scaling parameter in the proposal distribution of the hybrid SMH with new bounds is set to $\lambda = 0.5$ for SMH-1-NB and $\lambda = 1.5$ for SMH-2-NB. These values were chosen as they empirically maximise $\text{MSJD}/\mathbb{E}(B)$.

Panel (a) of Figure 7 demonstrates the substantial reduction in the subsample size that SMH can achieve when using our bounds. It also shows that, on average, SMH-NB with the first-order control variates requires smaller subsamples than MH-SS with the same approximation. This difference arises exclusively from the smaller scaling parameter in the proposal distribution of SMH-1-NB (i.e., $\lambda = 0.5$ for SMH-1-NB versus $\lambda = 1.5$ for MH-SS). In contrast, MH-SS-2 and SMH-2-NB have approximately the same $\mathbb{E}(B)$ since they share the same λ . A smaller λ implies smaller jumps from θ to θ' , negatively impacting efficiency metrics such as ESS since (when the acceptance rate is reasonable) a small λ tends to increase the correlation between successive values in the chain, especially in high-dimensional settings. For example, in panel (b) of Figure 7, both SMH-NB variants exhibit greater efficiency per second than their vanilla counterparts. However, each is consistently outperformed by the corresponding MH-SS algorithm, even though it shares the same bound, demonstrating superior performance of the algorithm itself, as well as the bounds.

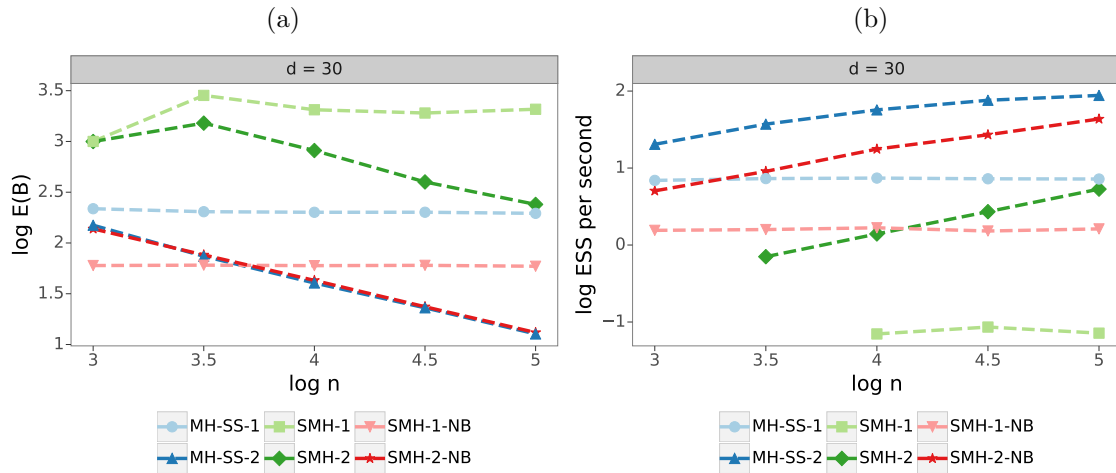


Figure 7: Average batch size and ESS per second for MH-SS, vanilla SMH and SMH with new bounds for the logistic regression model ($d = 30$). Both axes are presented in the logarithmic scale.

In summary, the results presented in Figure 7 suggest that SMH requires less data per iteration and has greater efficiency if it adopts tighter bounds. However, this is not sufficient to make

it at least as efficient as our proposed methods. Though SMH and MH-SS share similarities, such as the use of Poisson auxiliary variables and the assumption that the log-likelihood differences are bounded, the final algorithms are different. SMH, and especially SMH-1, suffers from its acceptance rate formulation as a product of individual acceptance probabilities. Moreover, SMH requires sampling up to $B - 1$ additional Bernoulli random variables per iteration.

5.3 Poisson regression

We now compare the MH-SS, Tuna, SMH and RWM algorithms using a set of synthetic data generated from a Poisson regression model with expectation $\log(1 + e^{x^\top \beta})$. We simulate synthetic datasets with $d = 30$, $n = (10^{4.5}, 10^5) = (31,622, 100,000)$ and sample the predictors and coefficients as for the logistic regression scenarios. For Tuna, we set (in the notation of [Zhang et al. \(2020\)](#)), $\chi = 2 \times 10^{-5}$ in both cases and $\lambda = 0.09$ for $n = 31,622$ and $\lambda = 0.05$ for $n = 100,000$. Following the suggestions of [Zhang et al. \(2020\)](#), these combinations lead to acceptance rates of approximately 60% and minimise the impact of χ on the average batch size.

Table 1 shows that MH-SS-1 and MH-SS-2 have the largest ESS per second. Once again, the empirical results for $\mathbb{E}(B)$ show that the SMH bounds scale poorly in moderate to high dimensions and that our proposed bounds are tighter. For instance, MH-SS-1 requires 14 times fewer observations than SMH-1, for $n = 31,622$, and it is slightly more efficient than SMH-2 in both scenarios. We note that the computational efficiency of SMH-1 is one of the lowest among the compared algorithms because, as pointed out in Section 3, it degrades quickly as d increases. Though Tuna requires on average the smallest subsample sizes per MCMC iteration, its efficiency is similar to that of the RWM. As already discussed, this low efficiency is due to the scaling parameter, λ , of the proposal distribution for Tuna being smaller than for any other algorithm, generating highly correlated posterior samples.

Table 1: Acceptance rate, average batch size, ESS per second and ESS/ $\mathbb{E}(B)$ for the Poisson regression model applied to synthetic data in $d = 30$. The values in bold denote the two largest efficiency metrics.

Model	Acc. rate	$\mathbb{E}(B)$	ESS per second	ESS/ $\mathbb{E}(B)$
$n = 31,622$				
Tuna	0.6051	100	0.04	0.02
MH-SS-1	0.4245	203	4.31	5.07
MH-SS-2	0.4505	19	60.91	56.42
SMH-1	0.1670	2,889	0.05	0.08
SMH-2	0.3184	256	4.29	5.11
RWM	0.2368	31,622	0.04	0.04
$n = 100,000$				
Tuna	0.6042	111	0.02	0.01
MH-SS-1	0.4229	195	6.57	5.43
MH-SS-2	0.4568	10	92.40	116.90
SMH-1	0.1630	2,773	0.05	0.08
SMH-2	0.3195	128	6.52	10.06
RWM	0.2384	100,000	0.01	0.01

6 Results on real datasets

In the simulation section, we showed that MH-SS outperforms the SMH, Tuna and RWM algorithms for different combinations of n and d using synthetic data. In this section, we extend our comparison using real-world datasets and three regression models: logistic, probit and Poisson with an expectation of $\log(1 + e^\eta)$, where η is the linear predictor. The objective is to illustrate that the MH-SS algorithm can be applied to the probit model, as well as in more challenging settings with larger n and correlated predictors which are not continuous and/or normally distributed. Results for the Tuna algorithm are not presented for the probit model as it is not possible to bound the first derivative of the log-likelihood of this model. We assess the algorithms in terms of computational efficiency, considering metrics including $\text{ESS}/\mathbb{E}(B)$ and ESS per second. We also present the empirical acceptance rates and average batch sizes. In all results presented in this section, the ESSs are at least 150 for all algorithms.

We first compare the methods on three binary datasets using the logistic and probit regression models only. Our fourth and last comparison uses a Poisson regression model on a dataset with $n = 298,290$ and $d = 28$. The first three datasets differ in many aspects, such as the numbers of observations and predictors as well the correlations between predictors. The later point is of particular interest as the simulation experiments only considered an intercept and continuous i.i.d. Gaussian predictors. Proposals are of the same form as in the Section 5, with V_d and λ set in the same way. For Tuna, we provide the values of λ and χ separately for each dataset.

We now point out aspects of the results common to all four analyses. Whether in terms of ESS per second or $\text{ESS}/\mathbb{E}[B]$, MH-SS-2 is always the most efficient algorithm. In terms of ESS per second, it is always at least an order of magnitude more efficient than any of the other algorithms. The second- and third-most efficient algorithms are always MH-SS-1 and SMH-2, though the order varies. MH-SS-2 always uses the fewest observations, but in all of the logistic regression models it is Tuna that uses the second fewest observations, and for the Poisson regression, it uses the third fewest observations. Despite the relatively low numbers of observations, Tuna always performs worse than either MH-SS-1 or SMH-2 (and often much worse than either) because the proposal scaling parameter is so small; see the discussion in Section 3.

6.1 U.S. Current Population Survey

We first illustrate the applicability of our method on the 2018 United States Current Population Survey (CPS; [Ruggles et al., 2024](#)). The CPS is a monthly household survey carried out by the U.S. Census Bureau and the U.S. Bureau of Labor Statistics that gathers information on the labour force for the population of the U.S. The data contain variables such as income, education, occupation, participation in welfare programs and health insurance. Using a sample of $n = 500,000$ survey participants, we wish to model whether or not an individual has a total pre-tax personal income above \$25,000 for the previous year, based on 10 predictors. We fit the logistic and probit models with an intercept term and normalise the covariates to improve numerical stability, ensuring each has a mean of zero and variance of one. As some of the variables are categorical, the linear predictor contains $d = 31$ parameters (including the intercept). For the Tuna algorithm, we set $\chi = 10^{-5}$ and $\lambda = 0.019$.

Table 2 presents the results for acceptance rate, average batch size, ESS per second and ESS divided by $\mathbb{E}(B)$ for the Tuna, MH-SS, SMH and RWM algorithms. Whether for the logistic or probit models, SMH-1 is not a viable option compared to the RWM. Although SMH-1 uses approximately 10% of the data, its efficiency per second is less than that of the RWM. This

is due to its relatively low scaling parameter, λ , and the additional computational overheads compared with the vanilla RWM, due to it being a more complex algorithm, including sampling extra random variables and performing vector/matrix multiplications. We stress that in all of our implementations, operations that can be pre-computed to speed up both SMH and MH-SS are performed accordingly.

Table 2: Acceptance rate, average batch size, ESS per second and $\text{ESS}/\mathbb{E}(B)$ for the logistic and probit regression models applied to a sample of $n = 500,000$ participants of the U.S. CPS. The values in bold denote the two largest efficiency metrics.

Model	Algorithm	Acc. rate	$\mathbb{E}(B)$	ESS per second	$\text{ESS}/\mathbb{E}(B)$
Logistic	Tuna	0.5935	284	0.003	0.001
	MH-SS-1	0.4405	989	1.35	0.92
	MH-SS-2	0.4561	88	27.37	10.62
	SMH-1	0.1577	49,060	0.002	0.003
	SMH-2	0.3191	8,288	0.13	0.13
	RWM	0.2391	500,000	0.005	0.002
	MH-SS-1	0.4038	1,543	0.82	0.66
Probit	MH-SS-2	0.4108	71	31.32	14.58
	SMH-1	0.1397	57,846	0.0006	0.0005
	SMH-2	0.2758	5,076	0.05	0.028
	RWM	0.1933	500,000	0.0005	0.002

6.2 Detection of gas mixtures

We now apply the various MCMC sampling algorithms to a dataset available in the UCI machine learning repository (Kelly et al., 2024; Fonollosa et al., 2015) which gathers recordings of multiple chemical sensors used to detect gas mixtures at varying concentrations. Our goal is to predict for a sample of size $n = 250,000$ whether the concentration of Ethylene in the air, measured in parts per million, is above zero. Though we consider $d = 7$ continuous predictors only (including an intercept), each of which corresponds to a different model sensor, some of them are highly correlated. In practice, this correlation is expected to increase $\mathbb{E}(B)$ for SMH and MH-SS, thereby potentially reducing their computational efficiency relative to RWM. For the Tuna algorithm, we set $\chi = 7 \times 10^{-6}$ and $\lambda = 0.025$.

Table 3 presents the efficiency metrics for all algorithms applied to the logistic and probit models. Notably, for logistic regression, Tuna is not competitive with any of the algorithms, except for the RWM, SMH-2 uses, on average, 4 times more observations per MCMC iteration than MH-SS-2, while the ratio of the average batch sizes of SMH-1 and MH-SS-1 is only just over 2. We remind the reader that as $\mathbb{E}(B)$ is a function of the bound on the log-likelihood differences, the looser SMH bounds result in larger average batch sizes. For a reasonable acceptance rate, SMH-1 requires a smaller scaling than MH-SS-1; this mitigates against the difference in batch size but reduces the mixing of the MCMC chain. The patterns are similar for the probit model, except that the MH-SS algorithms are more than a factor of 30 times more efficient than their SMH counterparts.

Table 3: Acceptance rate, average batch size, ESS per second and $\text{ESS}/\mathbb{E}(B)$ for the logistic and probit regression models applied to the gas sensor dataset. The values in bold denote the two largest efficiency metrics.

Model	Algorithm	Acc. rate	$\mathbb{E}(B)$	ESS per second	$\text{ESS}/\mathbb{E}(B)$
Logistic	Tuna	0.6091	321	0.02	0.006
	MH-SS-1	0.4778	945	6.44	4.21
	MH-SS-2	0.4774	165	91.91	23.77
	SMH-1	0.4373	2,260	0.48	0.72
	SMH-2	0.3491	680	8.90	6.98
	RWM	0.2738	250,000	0.03	0.02
Probit	MH-SS-1	0.4153	1,338	3.53	2.98
	MH-SS-2	0.4142	103	100.74	38.77
	SMH-1	0.3792	2,715	0.05	0.66
	SMH-2	0.2869	382	3.14	12.15
	RWM	0.2308	250,000	0.002	0.02

6.3 High-energy particle physics

We apply the scalable MCMC algorithms to the Hepmass dataset (Whiteson, 2016) from the UCI machine learning repository. The dataset contains information about signatures of exotic particles obtained from a high-energy physics experiment. The binary response variable indicates whether a new particle of unknown mass is observed. The dataset has originally 26 continuous predictors and is split into a training set of 7 million observations and a test set of 3.5 million. To illustrate the applicability of the proposed methods, we compare the algorithms on a subsample of $n = 1,000,000$ observations from the training set. For Tuna, we set χ and λ to 10^{-5} and 0.013, respectively.

Table 4 summarises the results of acceptance rate, $\mathbb{E}(B)$, ESS per second and $\text{ESS}/\mathbb{E}(B)$ for the logistic and probit regression models applied to the Hepmass dataset. The efficiencies of the RWM, Tuna and SMH are all around two (or more) orders of magnitude smaller than those of SMH-2 and MH-SS-1, which themselves are at least an order of magnitude smaller than that of MH-SS-2.

Table 4: Acceptance rate, average batch size, ESS per second and $\text{ESS}/\mathbb{E}(B)$ for the logistic and probit regression models applied to the Hepmass dataset. The values in bold denote the two largest efficiency metrics.

Model	Algorithm	Acc. rate	$\mathbb{E}(B)$	ESS per second	$\text{ESS}/\mathbb{E}(B)$
Logistic	Tuna	0.5914	295	0.002	0.001
	MH-SS-1	0.4465	766	0.76	1.25
	MH-SS-2	0.4557	31	46.07	31.10
	SMH-1	0.1685	11,844	0.01	0.01
	SMH-2	0.3221	493	2.45	2.43
	RWM	0.2433	1,000,000	0.003	0.001
Probit	MH-SS-1	0.4125	1,031	0.71	1.01
	MH-SS-2	0.4215	18	48.67	55.93
	SMH-1	0.1529	15,374	0.001	0.012
	SMH-2	0.2852	261	0.84	4.66
	RWM	0.1992	1,000,000	0.0002	0.001

6.4 Reported road casualties in the UK

The UK Department for Transport publishes annual road safety statistics as part of the Statistics and Registration Service Act 2007. The data include the accident’s geographical coordinates, severity, speed limit of the road where the accident took place, details about the vehicles involved, weather conditions, road conditions, as well as time and date (Lovelace et al., 2019). We compare the performance of MH-SS, SMH and Tuna on the consolidated UK road casualties data from 2020 to 2022. We aim to model at the individual level of $n = 298,290$ accidents the number of casualties based on 8 predictors, of which 2 are continuous. In total, the linear predictor in our Poisson model with mean $\log(1 + e^\eta)$ has $d = 28$ parameters (including the intercept). For the Tuna algorithm, we set χ and λ to 10^{-7} and 0.19, respectively.

Table 5 shows results of acceptance rate, average batch size, ESS per second and $\text{ESS}/\mathbb{E}(B)$ for MH-SS, SMH and Tuna. As per the analyses presented above considering datasets with a binary response variable, it is possible to see that MH-SS-1 and MH-SS-2 are the algorithms that on average require the smallest number of data points per MCMC iteration. Unsurprisingly, both versions of MH-SS present the best results in terms of computational efficiency. Though Tuna and MH-SS-1 have similar average batch sizes, again the latter is significantly more efficient as shown by its ESS per second and $\text{ESS}/\mathbb{E}(B)$.

Table 5: Acceptance rate, average batch size, ESS per second and $\text{ESS}/\mathbb{E}(B)$ for a Poisson regression model applied to the UK road casualties dataset. The values in bold denote the two largest efficiency metrics.

Model	Algorithm	Acc. rate	$\mathbb{E}(B)$	ESS per second	$\text{ESS}/\mathbb{E}(B)$
Poisson	Tuna	0.5964	2,680	0.015	0.002
	MH-SS-1	0.4542	1,927	0.79	0.52
	MH-SS-2	0.4572	391	8.61	2.59
	SMH-1	0.1893	44,262	0.003	0.004
	SMH-2	0.3219	20,320	0.05	0.06
	RWM	0.2414	298,290	0.011	0.004

7 Discussion

Performing posterior sampling via MCMC on datasets with a large number of observations poses a significant challenge, particularly to traditional methods like the Metropolis–Hastings (MH) algorithm, which requires the evaluation of all likelihood terms at each iteration. This challenge has led Bayesian researchers to turn away from MCMC algorithms and to instead utilise approximate and biased inference schemes, such as variational inference, in order to approximate the posterior distribution. Current approaches in the scalable MCMC literature aim to alleviate the computational burden of applying MCMC on large data sets by either partitioning the data into batches and running independent MCMC on each partition, or employing data subsampling techniques. In this paper, we have presented a novel exact Metropolis–Hastings-based algorithm designed to scale posterior sampling for large datasets through data subsampling. Our approach assumes that the log-likelihood differences can be tightly bounded and introduces an auxiliary Poisson variable which allows us to extend the Metropolis–Hastings ratio so that not all observations are needed, thereby reducing the computational effort per iteration.

Several previous approaches that utilise subsampling techniques to scale MCMC to large datasets rely on either the log-likelihood or log-likelihood differences being bounded. These methods typ-

ically introduce auxiliary variables to simplify the posterior sampling. However, there have been two main drawbacks: i) the auxiliary variables can be sub-optimally designed, which hinders the efficiency of the algorithm, and ii) the bounds on the log-likelihood are not sufficiently tight, especially as the number of predictors, d , increases. In our work, we have overcome these limitations and enhanced the scalability of MCMC methods to large datasets.

Our auxiliary variable approach shares features with that in [Zhang et al. \(2020\)](#), using Poisson random variables whose expectation depends on both the current and proposed value. However, as seen in the experiments and real-world applications of Sections 5 and 6, the Tuna algorithm ([Zhang et al., 2020](#)) typically performs relatively poorly because it requires sub-optimal scaling of the Metropolis–Hastings proposal in order to control the acceptance rate. Our more general formulation, combined with the use of control variates, leads to orders of magnitude greater efficiency. The scalable Metropolis–Hastings algorithm ([Cornish et al., 2019](#)) uses the same generic form for the control variates as we do, but our bounds on the discrepancy between the control variate and the truth scale better with increasing dimension and this, together with the removal of the large product in the acceptance probability and another novel tightening, has a substantial impact on the overall efficiency. We also have provided guidelines on choosing the proposal scaling, λ , for MH-SS in the case where the Metropolis–Hastings proposal is that of a random-walk Metropolis algorithm: choose λ to target an empirical acceptance of around 0.452. This guidance has been verified empirically and holds whether using first- or second-order control variates.

The simulation experiments presented in Section 5 utilising synthetic data from logistic and Poisson regression models demonstrate that our proposed algorithms require much smaller average batch sizes than those in [Cornish et al. \(2019\)](#) and exhibit consistently greater computational efficiency per second across various combinations of number of data points, n , and number of predictors, d . The real-world applications in Section 6, featuring datasets with observations ranging from $n = 250,000$ to $n = 1,000,000$ and three models (logistic, probit and Poisson regressions), show that i) our algorithms are highly efficient even in settings characterised by large n and correlated and/or categorical predictors and that ii) the RWM, SMH and TunaMH algorithms do not scale as well as MH-SS, and MH-SS-2 in particular.

References

- Andersen, M., Winther, O., Hansen, L. K., Poldrack, R., and Koyejo, O. (2018). Bayesian structure learning for dynamic brain connectivity. In *International Conference on Artificial Intelligence and Statistics*, pages 1436–1446. PMLR.
- Andrieu, C. and Roberts, G. O. (2009). The pseudo-marginal approach for efficient Monte Carlo computations. *The Annals of Statistics*, 37(2):697 – 725.
- Bardenet, R., Doucet, A., and Holmes, C. (2014). Towards scaling up Markov chain Monte Carlo: an adaptive subsampling approach. In *International Conference on Machine Learning*, pages 405–413. PMLR.
- Bardenet, R., Doucet, A., and Holmes, C. (2017). On Markov chain Monte Carlo methods for tall data. *Journal of Machine Learning Research*, 18(47).
- Beaumont, M. A. (2003). Estimation of population growth or decline in genetically monitored populations. *Genetics*, 164(3):1139–1160.
- Bierkens, J., Fearnhead, P., and Roberts, G. (2019). The Zig-Zag process and super-efficient sampling for Bayesian analysis of big data. *The Annals of Statistics*, 47(3):1288 – 1320.

- Böhning, D. (1999). The lower bound method in probit regression. *Computational Statistics & Data Analysis*, 30(1):13–17.
- Bouchard-Côté, A., Vollmer, S. J., and Doucet, A. (2018). The bouncy particle sampler: A nonreversible rejection-free Markov chain Monte Carlo method. *Journal of the American Statistical Association*, 113(522):855–867.
- Brooks, S., Gelman, A., Jones, G., and Meng, X.-L. (2011). *Handbook of Markov Chain Monte Carlo*. CRC press.
- Christen, J. A. and Fox, C. (2005). Markov chain Monte Carlo using an approximation. *Journal of Computational and Graphical Statistics*, 14(4):795–810.
- Cornish, R., Vanetti, P., Bouchard-Côté, A., Deligiannidis, G., and Doucet, A. (2019). Scalable Metropolis-Hastings for exact Bayesian inference with large datasets. In *International Conference on Machine Learning*, pages 1351–1360. PMLR.
- Cui, T., Fox, C., and O’sullivan, M. (2011). Bayesian calibration of a large-scale geothermal reservoir model by a new adaptive delayed-acceptance Metropolis-Hastings algorithm. *Water Resources Research*, 47(10).
- Fearnhead, P., Nemeth, C., Oates, C. J., and Sherlock, C. (2024). Scalable Monte Carlo for Bayesian learning. *arXiv preprint arXiv:2407.12751*.
- Fonollosa, J., Sheik, S., Huerta, R., and Marco, S. (2015). Reservoir computing compensates slow response of chemosensor arrays exposed to fast varying gas concentrations in continuous monitoring. *Sensors and Actuators B: Chemical*, 215:618–629.
- Gelman, A., Gilks, W. R., and Roberts, G. O. (1997). Weak convergence and optimal scaling of random-walk Metropolis algorithms. *The Annals of Applied Probability*, 7(1):110–120.
- Golightly, A., Henderson, D. A., and Sherlock, C. (2015). Delayed-acceptance particle MCMC for exact inference in stochastic kinetic models. *Statistics and Computing*, 25:1039–1055.
- Green, P. J. and Han, X.-l. (1992). Metropolis methods, Gaussian proposals and antithetic variables. In *Stochastic Models, Statistical Methods, and Algorithms in Image Analysis: Proceedings of the Special Year on Image Analysis, held in Rome, Italy, 1990*, pages 142–164. Springer.
- Kelly, M., Longjohn, R., and Nottingham, K. (2024). UCI machine learning repository.
- Korattikara, A., Chen, Y., and Welling, M. (2014). Austerity in MCMC land: Cutting the Metropolis-Hastings budget. In *International Conference on Machine Learning*, pages 181–189. PMLR.
- Lewis, P. W. and Shedler, G. S. (1979). Simulation of nonhomogeneous Poisson processes by thinning. *Naval Research Logistics Quarterly*, 26(3):403–413.
- Liu, J. S. and Chen, R. (1995). Blind deconvolution via sequential imputations. *Journal of the American Statistical Association*, 90(430):567–576.
- Liu, S., Mingas, G., and Bouganis, C.-S. (2015). An exact MCMC accelerator under custom precision regimes. In *2015 International Conference on Field Programmable Technology (FPT)*, pages 120–127. IEEE.

- Lovelace, R., Morgan, M., Hama, L., Padgham, M., Ranzolin, D., and Sparks, A. (2019). stats 19: A package for working with open road crash data. *The Journal of Open Source Software*, 4(33):1181.
- Maclaurin, D. and Adams, R. P. (2014). Firefly Monte Carlo: Exact MCMC with subsets of data. In *Proceedings of the 30th Conference on Uncertainty in Artificial Intelligence, Quebec City, Canada*, pages 543–552.
- Neiswanger, W., Wang, C., and Xing, E. (2013). Asymptotically exact, embarrassingly parallel MCMC. *arXiv preprint arXiv:1311.4780*.
- Nemeth, C. and Sherlock, C. (2018). Merging MCMC subposteriors through Gaussian Process approximations. *Bayesian Analysis*, 13(2):507 – 530.
- Peskun, P. H. (1973). Optimum Monte Carlo sampling using Markov chains. *Biometrika*, 60(3):607–612.
- Quiroz, M., Kohn, R., Villani, M., and Tran, M.-N. (2018a). Speeding up MCMC by efficient data subsampling. *Journal of the American Statistical Association*.
- Quiroz, M., Tran, M.-N., Villani, M., and Kohn, R. (2018b). Speeding up MCMC by delayed-acceptance and data subsampling. *Journal of Computational and Graphical Statistics*, 27(1):12–22.
- Raj, A., Stephens, M., and Pritchard, J. K. (2014). fastSTRUCTURE: variational inference of population structure in large SNP data sets. *Genetics*, 197(2):573–589.
- Ripley, B. D. (2009). *Stochastic simulation*. John Wiley & Sons.
- Robbins, H. and Monro, S. (1951). A stochastic approximation method. *The Annals of Mathematical Statistics*, pages 400–407.
- Robert, C. P., Casella, G., and Casella, G. (1999). *Monte Carlo statistical methods*, volume 2. Springer.
- Roberts, G. O. and Rosenthal, J. S. (2001). Optimal scaling for various Metropolis-Hastings algorithms. *Statistical Science*, 16(4):351–367.
- Ruggles, S., Flood, S., Sobek, M., Backman, D., Chen, A., Cooper, G., Richards, S., Rogers, R., and Schouweiler, M. (2024). IPUMS USA: Version 15.0 [dataset]. *IPUMS*.
- Sampford, M. R. (1953). Some inequalities on Mill’s ratio and related functions. *The Annals of Mathematical Statistics*, 24(1):130–132.
- Scott, S. L., Blocker, A. W., Bonassi, F. V., Chipman, H. A., George, E. I., and McCulloch, R. E. (2016). Bayes and big data: The consensus Monte Carlo algorithm. *International Journal of Management Science and Engineering Management*, 11:78–88.
- Sherlock, C., Golightly, A., and Henderson, D. A. (2017). Adaptive, delayed-acceptance MCMC for targets with expensive likelihoods. *Journal of Computational and Graphical Statistics*, 26(2):434–444.
- Sherlock, C. and Roberts, G. (2009). Optimal scaling of the random-walk Metropolis on elliptically symmetric unimodal targets. *Bernoulli*, 15(3):774 – 798.
- Sherlock, C., Thiery, A. H., and Golightly, A. (2021). Efficiency of delayed-acceptance random walk Metropolis algorithms. *The Annals of Statistics*, 49(5):2972 – 2990.

- Tierney, L. (1998). A note on Metropolis-Hastings kernels for general state spaces. *Annals of Applied Probability*, pages 1–9.
- Trojan, C., Fearnhead, P., and Nemeth, C. (2024). Diffusion generative modelling for divide-and-conquer MCMC. *arXiv preprint arXiv:2406.11664*.
- Van Rossum, G. and Drake, F. L. (2009). *Python 3 Reference Manual*. CreateSpace, Scotts Valley, CA.
- Vyner, C., Nemeth, C., and Sherlock, C. (2023). Swiss: A scalable Markov chain Monte Carlo divide-and-conquer strategy. *Stat*, 12(1):e523.
- Whiteson, D. (2016). HEPMASS. UCI Machine Learning Repository.
- Winter, S., Campbell, T., Lin, L., Srivastava, S., and Dunson, D. B. (2024). Emerging directions in Bayesian computation. *Statistical Science*, 39(1):62–89.
- Yogatama, D., Wang, C., Routledge, B. R., Smith, N. A., and Xing, E. P. (2014). Dynamic language models for streaming text. *Transactions of the Association for Computational Linguistics*, 2:181–192.
- Yuan, W. and Wang, G. (2024). Markov chain Monte Carlo without evaluating the target: an auxiliary variable approach. *arXiv preprint arXiv:2406.05242*.
- Zhang, R., Cooper, A. F., and De Sa, C. M. (2020). Asymptotically optimal exact minibatch Metropolis-Hastings. *Advances in Neural Information Processing Systems*, 33:19500–19510.

A Proof of theoretical results for MH-SS

A.1 Proof of Theorem 1

Proof: Theorem 1 relies on a preliminary result:

Proposition 1. For any $c > 0$, $\Delta \in \mathbb{R}$ and $\psi > 0$, let $E(\psi) := \mathbb{E} \left[1 \wedge c \left(\frac{\psi - \Delta}{\psi} \right)^S \right]$, where $S \sim \text{Pois}(\psi)$. Then $\frac{dE}{d\psi} \geq 0$.

Proof of Proposition 1:

$$E(\psi) = \exp(-\psi) \sum_{s=0}^{\infty} \frac{\psi^s}{s!} \left\{ 1 \wedge c \left(\frac{\psi'}{\psi} \right)^s \right\} = \exp(-\psi) \sum_{s=0}^{\infty} \frac{1}{s!} \{\psi^s \wedge c(\psi - \Delta)^s\}.$$

Now,

$$a := \frac{d}{d\psi} \{\psi^s \wedge c(\psi - \Delta)^s\} = s\psi^{s-1} \mathbf{1}(\psi^s \leq c(\psi - \Delta)^s) + sc(\psi - \Delta)^{s-1} \mathbf{1}(\psi^s > c(\psi - \Delta)^s).$$

The quantity a is either $s\psi^{s-1}$ or $sc(\psi - \Delta)^{s-1}$ so is at least as large as the minimum of the two. Hence, for $s > 0$,

$$\frac{d}{d\psi} \{\psi^s \wedge c(\psi - \Delta)^s\} \geq s\{\psi^{s-1} \wedge c(\psi - \Delta)^{s-1}\}.$$

Thus

$$\frac{dE}{d\psi} \geq \exp(-\psi) \left[\sum_{s=1}^{\infty} \frac{s}{s!} \{\psi^{s-1} \wedge c(\psi - \Delta)^{s-1}\} - \sum_{s=0}^{\infty} \frac{1}{s!} \{\psi^s \wedge c(\psi - \Delta)^s\} \right] = 0.$$

proving Proposition 1. \square

The maximal value of ψ , therefore leads to the maximal value of $E(\psi)$.

Next, decompose the expectation over $S = (S_1, \dots, S_n)$ of the acceptance rate

$$\mathbb{E} [\alpha_2(\theta, \theta'; S_1, \dots, S_n)] = \mathbb{E} \left[\mathbb{E} \left[\mathbb{E} [\dots \mathbb{E} [\alpha_2(\theta, \theta'; S_1, \dots, S_n) | S_2, \dots, S_n] \dots | S_{n-1}, S_n] | S_n \right] \right].$$

Applying Proposition 1 recursively with $\psi = \phi_i$, $i = n, \dots, 1$, shows that $\mathbb{E} [\alpha_2(\theta, \theta'; S_1, \dots, S_n)]$ is maximised when ψ is maximised since each of the intermediate expectations is maximised when ψ is maximised.

Finally, defining Δ_i as in (4),

$$\frac{d}{d\gamma} \phi_i = \max[0, \Delta_i] - \min[0, \Delta_i] - c_i M(\theta, \theta') = |\Delta_i| - c_i M(\theta, \theta') \leq 0,$$

so $\mathbb{E} [\alpha_2(\theta, \theta', S)]$ is maximised when ϕ_i is maximised, which is at $\gamma = 0$. \square

A.2 Proof of Theorem 2

A.2.1 Preliminaries

Lemma 2 (Mean-Value Theorem for $a : \mathbb{R}^d \rightarrow \mathbb{R}$). Let $a : \mathbb{R}^d \rightarrow \mathbb{R}$ be once differentiable and let $x_A \in \mathbb{R}^d$ and $x_B \in \mathbb{R}^d$. Then $a(x_B) - a(x_A) = (x_B - x_A)^\top \nabla a(x')$ for some x' on the line

between x_A and x_B .

Proof: Let $x = (1 - t)x_A + tx_B$ and set $b(t) = a(x(t))$. The Mean-Value Theorem for the univariate function b gives $a(x_B) - a(x_A) = b(1) - b(0) = b'(t')$ for some $t' \in [0, 1]$. But

$$\frac{db}{dt} = \frac{d}{dt}a((1 - t)x_A + tx_B) = \sum_{i=1}^d \frac{dx_i}{dt} \Big|_{t=t'} \frac{da}{dx_i} \Big|_{t=t'} = (x_B - x_A)^\top \nabla a(x'),$$

where $x' = (1 - t')x_A + t'x_B$. \square

Next, recall the *trapezium rule*: $\int_a^b f(x)dx = \frac{1}{2}\{f(a) + f(b)\} + \frac{1}{12}(b - a)^3 f''(\xi)$, where $\xi \in [a, b]$. We will use a slightly different version.

Proposition 2. *If $f'(x)$ is Lipschitz with a Lipschitz constant of L , then*

$$\left| \int_a^b f(x)dx - \frac{1}{2}(b - a)\{f(a) + f(b)\} \right| \leq \frac{1}{12}(b - a)^3 L.$$

Proof: Let $I = \int_a^b (x - c)f'(x)dx$, where $c = (a + b)/2$. Then, integrating by parts,

$$I = [(x - c)f(x)]_a^b - \int_a^b f(x)dx = \frac{1}{2}(b - a)\{f(a) + f(b)\} - \int_a^b f(x)dx.$$

However,

$$\left| \int_a^b (x - c)f'(x)dx \right| = \left| \int_a^b (x - c)\{f'(x) - f'(c)\}dx \right| \leq L \int_a^b (x - c)^2 dx,$$

which evaluates to the required expression. \square

A.2.2 Proof of the theorem itself

Proof: We prove the implications (15) \implies (16) and (17) \implies (18); the other two results follow analogously.

Proof of (15) \implies (16): Lemma 2 gives $\ell(\theta') - \ell(\theta) = (\theta' - \theta)^\top \nabla \ell(\tilde{\theta})$, for some $\tilde{\theta}$ on the line between θ and θ' . So $\ell(\theta') - \ell(\theta) - r_1(\theta, \theta'; \hat{\theta}) = r'$, where $r' := (\theta' - \theta)^\top \left\{ \nabla \ell(\tilde{\theta}) - \nabla \ell(\hat{\theta}) \right\}$.

Let $a(x) := \{\nabla \ell(x)\}^\top (\theta' - \theta)$ and apply Lemma 2 again, to see that

$$r' = a(\tilde{\theta}) - a(\hat{\theta}) = (\tilde{\theta} - \hat{\theta})^\top \nabla a(\theta^*) = (\tilde{\theta} - \hat{\theta})^\top H(\theta^*)(\theta' - \theta).$$

for some θ^* on the line between $\tilde{\theta}$ and $\hat{\theta}$. From (15), therefore, $r' \leq |x^\top (\theta' - \theta)| |x^\top (\tilde{\theta} - \hat{\theta})| M$. Now, $\tilde{\theta} - \hat{\theta} = \gamma(\theta - \hat{\theta}) + (1 - \gamma)(\theta' - \hat{\theta})$ for some $\gamma \in [0, 1]$, so

$$|x^\top (\tilde{\theta} - \hat{\theta})| = \gamma |x^\top (\theta - \hat{\theta})| + (1 - \gamma) |x^\top (\theta' - \hat{\theta})| \leq \max \left(|x^\top (\theta - \hat{\theta})|, |x^\top (\theta' - \hat{\theta})| \right),$$

which leads to (16).

Proof of (17) \implies (18): Let $a = \theta$, $b = \theta'$ and $x \in [0, 1]$. Then $f(z) = (\theta' - \theta)^\top g(\theta + z(\theta' - \theta))$ is the component in the $\theta' - \theta$ direction of the derivative of ℓ along the line joining θ to θ' and where z gives the fraction of the total distance along the line. We also have

$$f'(z) = (\theta' - \theta)^\top H(\theta + z\{\theta' - \theta\})(\theta' - \theta),$$

and from (17)

$$|f'(z_2) - f'(z_1)| \leq |x^\top(\theta' - \theta)| |x^\top(\theta' - \theta)| |x^\top(\theta' - \theta)| L |z_2 - z_1|.$$

Thus f' is Lipschitz. Proposition 2 applied with $a = 0$ and $b = 1$ then gives

$$\left| \ell(\theta') - \ell(\theta) - \frac{1}{2}(\theta' - \theta) \{g(\theta) + g(\theta')\} \right| \leq \frac{L}{12} |x^\top(\theta' - \theta)|^3. \quad (20)$$

Now, first order Taylor expansion of the scalar $(\theta' - \theta)^\top g(u)$ around $u = \hat{\theta}$ gives

$$\begin{aligned} (\theta' - \theta)^\top g(\theta') &= (\theta' - \theta)^\top g(\hat{\theta}) + (\theta' - \theta)^\top H(\hat{\theta})(\theta' - \hat{\theta}) + (\theta' - \theta)^\top \{H(\eta') - H(\hat{\theta})\}(\theta' - \hat{\theta}), \\ (\theta' - \theta)^\top g(\theta) &= (\theta' - \theta)^\top g(\hat{\theta}) + (\theta' - \theta)^\top H(\hat{\theta})(\theta - \hat{\theta}) + (\theta' - \theta)^\top \{H(\eta) - H(\hat{\theta})\}(\theta - \hat{\theta}), \end{aligned}$$

where $\eta = t\theta + (1-t)\hat{\theta}$ and $\eta' = t'\theta' + (1-t')\hat{\theta}$ for $0 \leq t, t' \leq 1$. Thus

$$\frac{1}{2}(\theta' - \theta)^\top \{g(\theta) + g(\theta')\} - r_2(\theta, \theta') = r'',$$

where

$$r'' := \frac{1}{2}(\theta' - \theta) \{H(\eta') - H(\hat{\theta})\}(\theta' - \hat{\theta}) + \frac{1}{2}(\theta' - \theta) \{H(\eta) - H(\hat{\theta})\}(\theta - \hat{\theta}).$$

The triangle inequality combined with (17) then gives

$$|r''| \leq \frac{L}{2} |x^\top(\theta' - \theta)| + |x^\top(\theta - \hat{\theta})| |x^\top(\eta - \hat{\theta})| + \frac{L}{2} |x^\top(\theta' - \theta)| + |x^\top(\theta' - \hat{\theta})| |x^\top(\eta' - \hat{\theta})|.$$

However, η is on the line between θ and $\hat{\theta}$, so $|x^\top(\eta - \hat{\theta})| \leq |x^\top(\theta - \hat{\theta})|$, and similarly, $|x^\top(\eta' - \hat{\theta})| \leq |x^\top(\theta' - \hat{\theta})|$. Combining with (20) via the triangle inequality gives (18). \square

A.3 Proof of Lemma 1

Proof: Let $c > 0$. If $u \cdot x < 0$, set $u' \leftarrow -u$ else $u' \leftarrow u$. If $v \cdot x < 0$ set $v' \leftarrow -vc\|u\|/\|v\|$ else $v' \leftarrow cv\|u\|/\|v\|$. Then, since the geometric mean is bounded by the arithmetic mean,

$$\{(u' \cdot x)^k (v' \cdot x)\}^{1/(k+1)} \leq \frac{1}{k+1} \{ku' \cdot x + v' \cdot x\} = \frac{1}{k+1} (ku' + v') \cdot x \leq \frac{1}{k+1} \|ku' + v'\| \|x\|,$$

by the Cauchy-Schwarz inequality. For any vector z , define $\hat{z} := z/\|z\|$. Thus,

$$\begin{aligned} \{(u' \cdot x)^k (v' \cdot x)\}^{2/(k+1)} &\leq \frac{1}{(k+1)^2} \{k^2 \|u'\|^2 + \|v'\|^2 + 2ku' \cdot v'\} \|x\|^2 \\ &= \frac{\|u\|^2}{(k+1)^2} \{k^2 + c^2 + 2kc\hat{u}' \cdot \hat{v}'\} \\ &\leq \frac{\|u\|^2}{(k+1)^2} \{k^2 + c^2 + 2kc|\hat{u}' \cdot \hat{v}'|\}, \end{aligned}$$

where the penultimate line follows as $\|v'\| = c\|u'\|$. However,

$$(u' \cdot x)^k (v' \cdot x) = |u' \cdot x|^k |v' \cdot x| = c \frac{\|u\|}{\|v\|} |u \cdot x|^k |v \cdot x|$$

and $|\hat{u}' \cdot \hat{v}'| = |\hat{u} \cdot \hat{v}| = |\omega|$, so

$$\left\{ |u \cdot x|^k |v \cdot x| \right\}^{2/(k+1)} \leq \|u\|^{2k/(k+1)} \|v\|^{2/(k+1)} \|x\|^2 \frac{h_k(c)}{(k+1)^2},$$

where

$$h_k(c) := \frac{k^2 + c^2 + 2kc|\omega|}{c^{2/(k+1)}}.$$

This is true for all c , and so is true at the minimiser of $h_k(c)$, which solves $c^2 + (k-1)c|\omega| = k$ and is $c = c_k(\omega)$ as defined in the statement of the lemma. At $c = c_k(\omega)$,

$$k^2 + c^2 + 2kc|\omega| = k^2 + (k+1)c_k(\omega)|\omega| + k = (k+1) \{k + c_k(\omega)|\omega|\}.$$

Hence, the right hand side of the inequality is

$$\|u\|^{2k/(k+1)} \|v\|^{2/(k+1)} \|x\|^2 \frac{h_k(c_k(\omega))}{(k+1)^2} = \|u\|^{2k/(k+1)} \|v\|^{2/(k+1)} \|x\|^2 \frac{k + c_k(\omega)|\omega|}{(k+1)c_k(\omega)^{2/(k+1)}}.$$

Raising to the power of $(k+1)/2$ gives the required result. \square

A.4 Specifics for regression models

Theorem 3. *With a single observation y , for logistic regression $|\mathfrak{h}''(\eta)| \leq M_{\text{logit}}(y) = 1/4$ and $|\mathfrak{h}'''(\eta)| \leq L_{\text{logit}}(y) = \sqrt{3}/18$, for probit regression $|\mathfrak{h}''(\eta)| \leq M_{\text{probit}}(y) = 1$, and for Poisson regression with an expectation of $\log(1 + \lambda \exp(\eta))$, $|\mathfrak{h}''(\eta)| \leq M_{\text{Pois}}(y) = 0.25 + 0.168y$.*

Remark 3. *Plotting $\mathfrak{h}'''(\eta)$ for probit regression and the relevant portion of $\mathfrak{h}'''(\eta)$ for Poisson regression over a fine grid strongly suggests that for probit regression, $|\mathfrak{h}'''(\eta)| < L_{\text{probit}}(y) = 0.30$ and for Poisson regression, $|\mathfrak{h}'''(\eta)| < L_{\text{Pois}}(y) = \sqrt{3}/18 + 0.061y$; we do not formally prove these bounds.*

Proof: Logistic regression, $\mathfrak{h}(\eta) = y \log[p/(1-p)] + \log(1-p) = y\eta - \log(1 + \exp(\eta))$, so $\mathfrak{h}'(\eta) = y - \frac{\exp(\eta)}{1 + \exp(\eta)}$ and

$$-\mathfrak{h}''(\eta) = \frac{\exp(\eta)}{\{1 + \exp(\eta)\}^2} = p(1-p).$$

Hence, $0 \leq -\mathfrak{h}''(\eta) \leq 1/4$. Furthermore

$$\mathfrak{h}'''(\eta) = \frac{\exp(\eta) - \exp(2\eta)}{\{1 + \exp(\eta)\}^3}.$$

This is maximised at $\exp(\eta) = 2 - \sqrt{3}$ and minimised at $\exp(\eta) = 2 + \sqrt{3}$. Substitution gives $-\sqrt{3}/18 \leq \mathfrak{h}'''(\eta) \leq \sqrt{3}/18$. \square

Aside: Notice that $|\mathfrak{h}'(\eta)| = |y - p| \leq 1$. This leads to the Tuna bound (no control variates).

Probit regression, $\mathfrak{h}(\eta) = y \log \Phi(\eta) + (1-y) \log \Phi(-\eta)$,

$$\begin{aligned} \mathfrak{h}'(\eta) &= y \frac{\phi(\eta)}{\Phi(\eta)} - (1-y) \frac{\phi(\eta)}{\Phi(-\eta)}, \\ -\mathfrak{h}''(\eta) &= y\phi(\eta) \frac{\phi(\eta) + \eta\Phi(\eta)}{\Phi(\eta)^2} + (1-y)\phi(\eta) \frac{\phi(\eta) - \eta\Phi(-\eta)}{\Phi(-\eta)^2}. \end{aligned}$$

For $\mathfrak{h}''(\eta)$, $(y, \eta) \leftrightarrow (1-y, -\eta)$ switches the first and second terms, and only one of these terms

is ever non-zero, so it is sufficient to bound the first term.

$$T(\eta) = \phi(\eta) \frac{\phi(\eta) + \eta\Phi(\eta)}{\Phi(\eta)^2}.$$

We now show that $0 \leq T(\eta) \leq 1$ by showing that it is decreasing and finding the limits at $-\infty$ and ∞ ; from this, $0 \leq -\mathfrak{h}''(\eta) \leq 1$.

Firstly, set $g(\eta) = \phi(\eta)/\Phi(\eta) \geq 0$. Calculus gives:

$$T' = \frac{\phi(\eta)}{\Phi(\eta)^3} [1 - (\phi(\eta) + \eta\Phi(\eta))(2\phi(\eta) + \eta\Phi(\eta))] = g(\eta) [1 - (g(\eta) + \eta)(2g(\eta) + \eta)].$$

Equation (4) and Section 3 of [Sampford \(1953\)](#) shows that $g(-\eta)[(g(-\eta)-\eta)(2g(-\eta)-\eta)-1] > 0$ for all η ; hence $T'(\eta) < 0$ for all η .

Next, we write $T(\eta) = T_1(\eta)T_2(\eta)$, where $T_1(\eta) = \frac{\phi(\eta)/\eta}{\Phi(\eta)}$ and $T_2(\eta) = \frac{\eta\phi(\eta) + \eta^2\Phi(\eta)}{\Phi(\eta)}$. Applying l'Hopital's rule to T_1 gives

$$\lim_{\eta \rightarrow -\infty} T_1(\eta) = \lim_{\eta \rightarrow -\infty} \frac{-\phi(\eta) - \phi(\eta)/\eta^2}{\phi(\eta)} = -1.$$

Applying l'Hopital to T_2 gives

$$\lim_{\eta \rightarrow -\infty} T_2(\eta) = \lim_{\eta \rightarrow -\infty} \frac{-\eta^2\phi(\eta) + \phi(\eta) + \eta^2\Phi(\eta) + 2\eta\Phi(\eta)}{\phi(\eta)} = 1 + 2 \lim_{\eta \rightarrow -\infty} \frac{1}{T_1(\eta)} = -1.$$

So $\lim_{\eta \rightarrow -\infty} T(\eta) = 1$.

Finally, as $\eta \rightarrow \infty$, $\Phi(\eta) \rightarrow 1$ and both $\phi(\eta)$ and $\eta\phi(\eta) \rightarrow 0$, so $T(\eta) \rightarrow 0$. \square

Note: [Böhning \(1999\)](#) gives the same bound, but does not prove the monotonicity between the limits as $\eta \rightarrow \pm\infty$.

Poisson regression: Setting $\eta' = \eta + \log \lambda$, $d\mathfrak{h}/d\eta = d\mathfrak{h}/d\eta' \times d\eta'/d\eta = d\mathfrak{h}/d\eta'$, so without loss of generality we may set $\lambda = 1$. Now, $\mathfrak{h} = y \log \log[1 + \exp(\eta)] - \log(1 + \exp(\eta)) - \log(y!)$,

$$\mathfrak{h}'(\eta) = y \frac{1}{\log[1 + \exp(\eta)]} \frac{\exp(\eta)}{1 + \exp(\eta)} - \frac{\exp(\eta)}{1 + \exp(\eta)}, \quad (21)$$

$$-\mathfrak{h}''(\eta) = \frac{\exp(\eta)}{\{1 + \exp(\eta)\}^2} \left[y \left\{ \frac{\exp(\eta)}{\{\log(1 + \exp(\eta))\}^2} - \frac{1}{\log(1 + \exp(\eta))} \right\} + 1 \right]. \quad (22)$$

Set

$$0 \leq S(\eta) := \frac{\exp(\eta)}{\{1 + \exp(\eta)\} \log(1 + \exp(\eta))} \leq 1,$$

as $\log(1 + x) \geq x/(x + 1)$ for all $x > -1$. The coefficient of y in $-\mathfrak{h}''(\eta)$ can be written as $S(\eta)R(\eta)$, where

$$R(\eta) = S(\eta) - 1/(1 + \exp(\eta)) \geq 0,$$

since $\log(1 + x) \leq x$.

Firstly, by Taylor expansion, $\log(1 + \exp(x)) \geq \exp(x) - \frac{1}{2} \exp(2x)$, so, for $\eta < 0$,

$$R(\eta) \leq \frac{1}{\{1 + \exp(\eta)\} \{1 - \frac{1}{2} \exp(\eta)\}} - \frac{1}{1 + \exp(\eta)} = \frac{\exp(\eta)}{2 + \exp(\eta) - \exp(2\eta)} \leq \frac{1}{2} \exp(\eta).$$

Thus, for $\eta \leq -\log 3$, $S(\eta)R(\eta) \leq R(\eta) \leq R(-\log 3) \leq 1/6$.

Secondly, $\log(1+x) > \log(x)$, so

$$R(\eta) \leq \frac{\exp(\eta)}{\eta\{1+\exp(\eta)\}} - \frac{1}{1+\exp(\eta)} = \frac{1}{\eta\{1+\exp(-\eta)\}} - \frac{1}{1+\exp(\eta)} \leq \frac{1}{\eta}.$$

Hence, for $\eta \geq 6$, $S(\eta)R(\eta) \leq R(\eta) \leq R(6) \leq 1/6$.

Next, we numerically maximise $S(\eta)R(\eta)$ on the interval $[-\log 3, 6]$ to obtain $SR < 0.168$.

Finally, the term that does not involve y is positive, with a magnitude of at most $1/4$, which leads to the bound.

Aside: To obtain the bounds for the Tuna algorithm (Zhang et al., 2020), it is needed to bound $|\mathfrak{h}'(\eta)|$. Applying l'Hopital's rule to the coefficient of y_i in $\mathfrak{h}'(\eta)$ (21), $S(\eta)$, gives

$$\lim_{\eta \rightarrow \infty} S(\eta) = 0 \quad \text{and} \quad \lim_{\eta \rightarrow -\infty} S(\eta) = 1,$$

and the limits of the second term in $\mathfrak{h}'(\eta)$ are 0 and -1 as η goes to $-\infty$ and ∞ , respectively. So,

$$\lim_{\eta \rightarrow \infty} \mathfrak{h}'(\eta) = -1 \quad \text{and} \quad \lim_{\eta \rightarrow -\infty} \mathfrak{h}'(\eta) = y.$$

Using $\log(1+\exp(\eta)) < \exp(\eta)$ for all η , the coefficient of y_i in (22) is always positive. Thus, $\mathfrak{h}''(\eta) < 0$ for all η and $\mathfrak{h}'(\eta)$ is decreasing and hence lies between its limits, -1 and y . So, $|\mathfrak{h}'(\eta)| \leq \max(1, y)$. \square

B Asymptotic analysis of bounds

We first analyse the tightness of the bounds from Theorem 2 and then incorporate the computational cost of evaluating the bounds under the assumption that the cost of evaluating the likelihood $\ell_i(\theta)$ is $\mathcal{O}(d)$. We compare the costs to those of the SMH algorithm (Cornish et al., 2019).

In regression examples with each $\beta_j \sim \mathbf{N}(0, 1)$, $j = 1, \dots, d$, independently, we sampled covariates

$$x_{i,j} \sim \mathbf{N}(0, 1/d), \quad i = 1, \dots, n, \quad j = 2, \dots, d, \quad (23)$$

independently, with $x_{i,1} = 1$. The variance was chosen so that the linear predictor, $x_i^\top \beta$ remains $\mathcal{O}(1)$ as d increases.

We find that the overall costs of evaluating our algorithm's accept-reject probability using $r^{(1)}$ is $\mathcal{O}(d^{3/2})$, which is independent of n , whereas for $r^{(2)}$ the cost is $\mathcal{O}(d^3 n^{-1/2})$. The cost of the SMH algorithm depends on the distribution of the covariates used. If (as in our simulations) these are Gaussian, then each iteration of the SMH-1 algorithm costs $\mathcal{O}(d^2 \log d)$, and for SMH-2 the cost is $\mathcal{O}(d^{7/2} \{\log d\}^{3/2} n^{-1/2})$; the terms in $\log d$ vanish if the covariates are bounded and the terms become larger if the covariates have heavier-than-Gaussian tails. For reference, the RWM costs $\mathcal{O}(dn)$: reductions in the cost per-data point come at the expense of increasing cost with dimension.

Assumptions: We assume the following:

- The Bernstein-von Mises limit applies and so

$$\theta \sim \mathbf{N}\left(\tilde{\theta}, \frac{1}{n} \mathbb{I}_{\mathbb{E}}^d(\theta_*)^{-1}\right), \quad (24)$$

where θ_* is the true parameter value and $\tilde{\theta}$ is the posterior mode. In regression models, for example, if the covariate vector $X_i \sim \nu$, for some distribution, ν , then $\mathbb{I}_{\mathbb{E}}^d(\theta_*) = \mathbb{E}_{X \sim \nu} [\mathbb{I}_{\mathbb{E}}^d(\theta_*; X)]$, the expectation over covariate vectors of the expected Fisher information conditional on the covariates.

- We consider the RWM, with a proposal of $\theta' \sim \mathbf{N}(\theta, \lambda_{n,d}^2 V^d)$ for some fixed (as n increases) positive-definite matrix, V^d .
- We assume that $\Sigma^d := \mathbb{I}_{\mathbb{E}}^d(\theta_*)^{-1}$ is well behaved as $d \rightarrow \infty$, satisfying the conditions in (25) and that the user ensures that V^d is similarly well-behaved, satisfying (26):

$$\frac{1}{d} \text{trace}(\Sigma^d) \rightarrow t_\pi < \infty, \quad \frac{1}{d} \sum_{i=1}^d \left(\Sigma_{i,i}^d \right)^{1/2} \rightarrow t_\pi^* > 0 \quad \text{and} \quad \frac{1}{d^2} \sum_{i=1, j=1}^{d,d} \left(\Sigma_{i,j}^d \right)^2 \rightarrow 0, \quad (25)$$

$$\frac{1}{d} \text{trace}(V^d) \rightarrow t_v < \infty, \quad \frac{1}{d} \sum_{i=1}^d \left(V_{i,i}^d \right)^{1/2} \rightarrow t_v^* > 0 \quad \text{and} \quad \frac{1}{d^2} \sum_{i=1, j=1}^{d,d} \left(V_{i,j}^d \right)^2 \rightarrow 0. \quad (26)$$

- To keep the acceptance rate bounded as n and d become large, we choose

$$\lambda_{n,d} = \frac{\ell}{n^{1/2} d^{1/2}}. \quad (27)$$

The function of n follows directly from (24), whereas the function of d follows from Gelman et al. (1997) and the many subsequent articles on optimal scaling of the random walk Metropolis algorithm.

- We assume that $\hat{\theta}$, the approximation to the mode, found via a stochastic-gradient algorithm, satisfies:

$$\|\hat{\theta} - \tilde{\theta}\|_2 \leq c \frac{d^{1/2}}{n^{1/2}}, \quad (28)$$

for some $c < t_\pi$ and not depending on n or d . This assumption is weak: in practice, for a reasonable approximation to the mode, we would expect $c \ll t_\pi$.

Proposition 3. *Subject to assumptions (24), (25), (26), (28) and (27):*

$$\begin{aligned} \|\theta' - \theta\|_2 &= \Theta(n^{-1/2}), \quad \|\theta - \hat{\theta}\|_2 = \Theta(d^{1/2} n^{-1/2}) \quad \text{and} \quad \|\theta' - \hat{\theta}\|_2 = \Theta(d^{1/2} n^{-1/2}), \\ \mathbb{E} [\|\theta' - \theta\|_1] &= \Theta(d^{1/2} n^{-1/2}), \quad \mathbb{E} [\|\theta - \hat{\theta}\|_1] = \Theta(dn^{-1/2}) \quad \text{and} \quad \mathbb{E} [\|\theta' - \hat{\theta}\|_1] = \Theta(dn^{-1/2}), \\ \|\theta' - \theta\|_1 &= \mathcal{O}(d^{1/2} n^{-1/2}), \quad \|\theta - \hat{\theta}\|_1 = \mathcal{O}(dn^{-1/2}) \quad \text{and} \quad \|\theta' - \hat{\theta}\|_1 = \mathcal{O}(dn^{-1/2}). \end{aligned}$$

Proof: We will use the following repeatedly: for any vector $A \sim \mathbf{N}(0, W)$ for some positive definite matrix W :

$$\mathbb{E} \left[\sum_{i=1}^d A_i^2 \right] = \text{trace}(W), \quad \text{Var} \left[\sum_{i=1}^d A_i^2 \right] = 2 \sum_{i,j=1}^{d,d} W_{i,j}^2, \quad \mathbb{E} \left[\sum_{i=1}^d |A_i| \right] = \sqrt{\frac{2}{\pi}} \sum_{i=1}^d \sqrt{W_{i,i}}.$$

From (26) and (27), as $d \rightarrow \infty$, for any fixed n ,

$$\begin{aligned} \mathbb{E} [n \|\theta' - \theta\|_2^2] &= n \lambda_{n,d}^2 \text{trace}(V_d) \rightarrow \ell^2 t_v, \\ \text{Var} [n \|\theta' - \theta\|_2^2] &\rightarrow 0, \end{aligned}$$

so $n \|\theta' - \theta\|_2^2 \rightarrow \ell^2 t_v$ almost surely, giving the bound for $\|\theta' - \theta\|_2$. Analogously, $n \|\theta - \hat{\theta}\|_2^2 / d \rightarrow t_\pi$

almost surely, so, by the triangle inequality,

$$\frac{n^{1/2}}{d^{1/2}} \|\tilde{\theta} - \hat{\theta}\|_2 - \frac{n^{1/2}}{d^{1/2}} \|\theta - \tilde{\theta}\|_2 \leq \frac{n^{1/2}}{d^{1/2}} \|\theta - \hat{\theta}\|_2 \leq \frac{n^{1/2}}{d^{1/2}} \|\tilde{\theta} - \hat{\theta}\|_2 + \frac{n^{1/2}}{d^{1/2}} \|\theta - \tilde{\theta}\|_2.$$

In the limit as $d \rightarrow \infty$, and subject to (25) and (28), we obtain

$$t_\pi - c \leq \frac{n^{1/2}}{d^{1/2}} \|\theta - \hat{\theta}\|_2 \leq t_\pi + c,$$

giving the bounds for $\|\theta - \hat{\theta}\|_2$. The triangle inequality then gives

$$\|\theta - \hat{\theta}\|_2 - \|\theta' - \theta\|_2 \leq \|\theta' - \hat{\theta}\|_2 \leq \|\theta - \hat{\theta}\|_2 + \|\theta' - \theta\|_2,$$

giving the bounds for $\|\theta' - \hat{\theta}\|_2$.

For the L_1 norms, by Jensen's inequality,

$$\|A\|_1 = \sum_{i=1}^d |A_i| = d \frac{1}{d} \sum_{i=1}^d |A_i| \leq d \sqrt{\frac{1}{d} \sum_{i=1}^d A_i^2} = d^{1/2} \|A\|_2.$$

We already know the limiting L_2 norms of $\theta' - \theta$, $\theta - \hat{\theta}$ and $\theta' - \hat{\theta}$ so we know that the limiting L_1 norms can be no more than a factor $d^{1/2}$ larger. However,

$$\frac{n^{1/2}}{d^{1/2}} \mathbb{E} [\|\theta' - \theta\|_1] = \frac{n^{1/2}}{d^{1/2}} \sqrt{\frac{2}{\pi}} \frac{\ell}{n^{1/2} d^{1/2}} \sum_{i=1}^d \sqrt{V_{ii}} = \sqrt{\frac{2}{\pi}} \frac{\ell}{d} \sum_{i=1}^d \sqrt{V_{ii}} \rightarrow \ell \sqrt{\frac{2}{\pi}} t_v^*.$$

Similarly

$$\frac{n^{1/2}}{d} \mathbb{E} [\|\theta - \hat{\theta}\|_1] = \frac{n^{1/2}}{d} \sqrt{\frac{2}{\pi}} \frac{1}{\sqrt{n}} \sum_{i=1}^d \sqrt{\Sigma_{ii}} = \sqrt{\frac{2}{\pi}} \frac{1}{d} \sum_{i=1}^d \sqrt{V_{ii}} \rightarrow \sqrt{\frac{2}{\pi}} t_\pi^*.$$

The triangle inequality shows that $\mathbb{E} [\|\theta' - \hat{\theta}\|_1]$ behaves similarly to $\mathbb{E} [\|\theta - \hat{\theta}\|_1]$. \square

B.1 Our bounds

For each observation, we now apply Proposition 3 to the generic bounds from Theorem 2, (16) and (18) passed through Lemma 1. From (23), we also have that $\|x_i\|_2 = o(1)$. Given $\Theta(\|\theta' - \theta\|_2) < \Theta(\|\theta - \hat{\theta}\|_2) = \Theta(\|\theta' - \hat{\theta}\|_2)$,

$$\begin{aligned} \left| \ell(\theta') - \ell(\theta) - r^{(1)}(\theta, \theta'; \hat{\theta}) \right| &\leq \Theta(\|\theta' - \theta\|_2) \Theta(\|\theta - \hat{\theta}\|_2) = \Theta(n^{-1/2}) \Theta(d^{1/2} n^{-1/2}) = \Theta(d^{1/2} n^{-1}), \\ \left| \ell(\theta') - \ell(\theta) - r^{(2)}(\theta, \theta'; \hat{\theta}) \right| &\leq \Theta(\|\theta' - \theta\|_2) \Theta(\|\theta - \hat{\theta}\|_2^2) = \Theta(n^{-1/2}) \Theta(d^{1/2} n^{-1/2})^2 = \Theta(d n^{-3/2}). \end{aligned}$$

The above bounds are proportional to the probability that a given observation will be used in the accept reject stage. There are n observations, and evaluation of each $r_i^{(1)}$ is $\Theta(d)$, so the overall costs of $r^{(1)}$ is $n \times \Theta(d^{1/2} n^{-1}) \times \Theta(d) = \mathcal{O}(d^{3/2})$. In general, evaluation of each $r_i^{(2)}$ has a cost of $\Theta(d^2)$. Hence the cost for $r^{(2)}$ is $n \times \Theta(d n^{-3/2}) \times \Theta(d^2) = \Theta(d^3/n^{1/2})$.

B.2 SMH bounds

For the SMH algorithm, Equation (13) of [Cornish et al. \(2019\)](#) has

$$\begin{aligned} \left| \ell_i(\theta') - \ell_i(\theta) - r_i^{(1)}(\theta, \theta'; \hat{\theta}) \right| &\leq \frac{1}{2} \left(\|\theta - \hat{\theta}\|_1^2 + \|\theta' - \hat{\theta}\|_1^2 \right) \bar{U}_{2,i}, \\ \left| \ell_i(\theta') - \ell_i(\theta) - r_i^{(2)}(\theta, \theta'; \hat{\theta}) \right| &\leq \frac{1}{6} \left(\|\theta - \hat{\theta}\|_1^3 + \|\theta' - \hat{\theta}\|_1^3 \right) \bar{U}_{3,i}, \end{aligned}$$

where

$$\bar{U}_{2,i} = \max_{j,k=1,\dots,d} \sup_{\theta \in \Theta} \left| \frac{\partial^2 U_i}{\partial \theta_j \partial \theta_k} \right| \quad \text{and} \quad \bar{U}_{3,i} = \max_{j,k,l=1,\dots,d} \sup_{\theta \in \Theta} \left| \frac{\partial^3 U_i}{\partial \theta_j \partial \theta_k \partial \theta_l} \right|$$

Repeating the total cost analysis, including the $\mathcal{O}(d)$ cost of evaluating $r^{(1)}$ and the $\mathcal{O}(d^2)$ cost for $r^{(2)}$, for the scalable MH bounds, we obtain costs of $\mathcal{O}(d^3 n^{-1}) \sum_{i=1}^n \bar{U}_{2,i}$ and $\mathcal{O}(d^5 n^{-3/2}) \sum_{i=1}^n \bar{U}_{3,i}$ for first and second-order control variates, respectively.

For the logistic regression model, Appendix G.1 of the SMH paper ([Cornish et al., 2019](#)) derives $\bar{U}_{2,i} = \frac{1}{4} \max_{1 \leq j \leq d} |x_{i,j}|^2$ and $\bar{U}_{3,i} = \frac{1}{6\sqrt{3}} \max_{1 \leq j \leq d} |x_{i,j}|^3$. Thus, if $d^{1/2} x_{i,j}$ is bounded, so are $d \bar{U}_{2,i}$ and $d^{3/2} \bar{U}_{3,i}$. If, on the other hand, each $x_{i,j}$ is Gaussian then $\bar{U}_{2,i} = \mathcal{O}(d^{-1} \log d)$ and $\bar{U}_{3,i} = \mathcal{O}(d^{-3/2} \{\log d\}^{3/2})$. In this case, we have total computational costs of $\mathcal{O}(d^2 \log d)$ for SMH-1 and $\mathcal{O}(d^{7/2} \{\log d\}^{3/2} n^{-1/2})$ for SMH-2.

C Additional simulation experiments

In this section, we present additional comparisons using $\text{ESS}/\mathbb{E}(B)$ as an efficiency metric. Figure 8 shows that the MH-SS algorithms consistently outperform SMH, Tuna and the RWM in terms of $\text{ESS}/\mathbb{E}(B)$. Notably, the efficiency gap between MH-SS-1 and SMH-1 is more pronounced compared to MH-SS-2 and SMH-2, especially as d increases. This discrepancy can be attributed to two main factors. Firstly, the bounds on the log-likelihood differences in MH-SS-1 are significantly tighter than those in SMH-1, as demonstrated in Section 4 and Appendix B. Tighter bounds result in a smaller $\mathbb{E}(B)$. Secondly, the acceptance rates of SMH-1 deteriorate drastically as d increases, as discussed in Section 3, whereas they tend to remain stable for SMH-2. As efficiency metrics like ESS take into account the autocorrelation of the posterior samples, lower acceptance rates lead to smaller ESS. In summary, the results for SMH-1 are influenced by a combination of loose bounds and poor acceptance rates, especially in high-dimensional settings.

C.1 Comparison of implementations

The results presented throughout the paper consider an implementation of SMH that evaluates the likelihood at most $B \leq n$ times in each MCMC iteration. If the proposal θ' is accepted, it indicates that the likelihood was exactly evaluated B times. Conversely, if θ' is rejected, it suggests that the likelihood was most likely evaluated fewer than B times because SMH is designed to reject a proposal based on sequential point-wise likelihood evaluations; for more details, see Algorithm 1 in [Cornish et al. \(2019\)](#). In contrast, both MH-SS and Tuna are originally designed to evaluate the likelihood exactly B times before deciding whether to accept or reject the proposal.

The sequential point-wise rejection process employed by SMH implies that likelihood evaluations cannot be computed in a vectorised fashion in programming languages like Python and R.

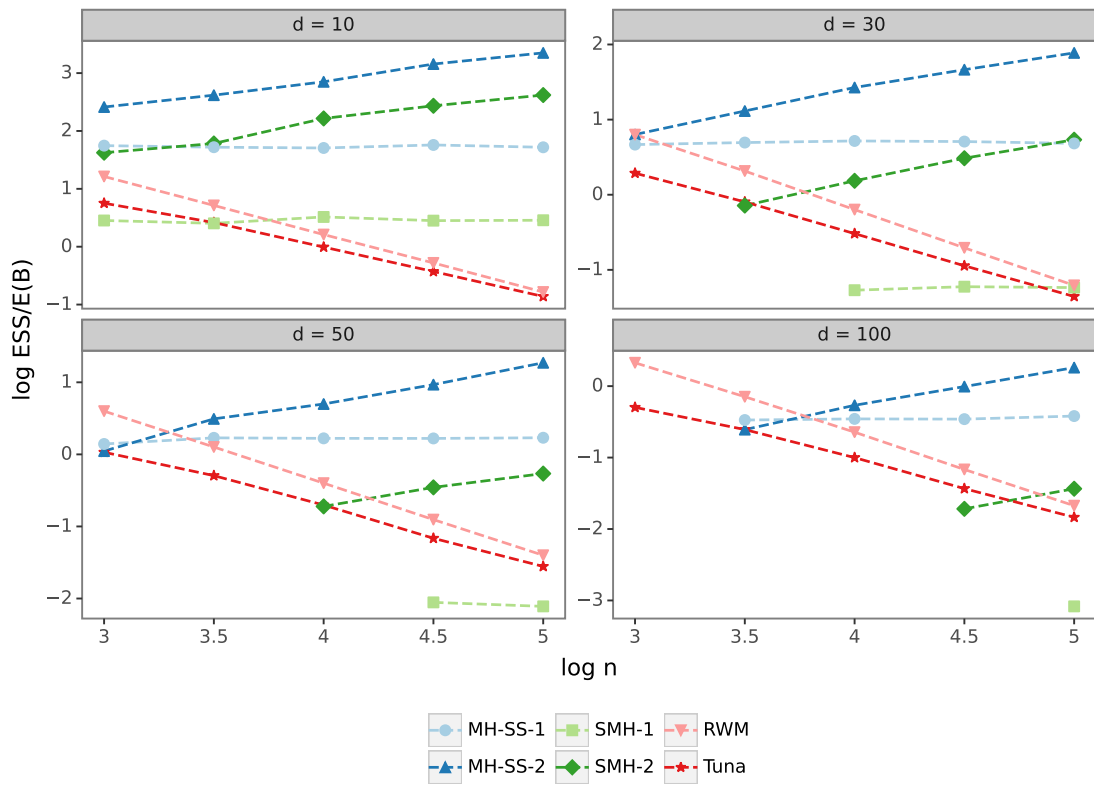


Figure 8: ESS divided by $\mathbb{E}(B)$ for MH-SS, SMH and RWM for the logistic regression model. Both axes are presented in the logarithm base 10. Some ESSs are omitted because $\mathbb{E}(B) \geq n$, which implies the use of the RWM algorithm.

Consequently, while loops are required to handle these evaluations. We point out that, for the sake of fair run-time comparisons, the results presented in the paper for RWM, SMH, MH-SS and Tuna were all obtained from implementations based on for-loops. In practice, however, we find that vectorised operations in Python are often faster compared to those relying on for-loops.

In an effort to enhance the run-time efficiency of SMH, we implemented a vectorised approach for evaluating the likelihood. For fairness in the comparisons, when vectorising the loops in SMH-1 and SMH-2, we also vectorised the computations in Tuna, MH-SS-1, MH-SS-2 and in the RWM. In the ‘vectorised SMH’ algorithm, the likelihood is evaluated exactly B times regardless of whether θ' is accepted or rejected. We note that the impact of SMH vectorization is exclusively observed in metrics related to run-times, such as ESS per second. Specifically, only the denominator of the ESS per second changes, as the ESS remains the same. Metrics like $\mathbb{E}(B)$ and $\text{ESS}/\mathbb{E}(B)$ also remain the same. Though this modification resulted in a significant computational speed-up, particularly for SMH-1 as it tends to evaluate more likelihood terms, it was not enough to make SMH more computationally efficient than MH-SS.

Figure 9 shows the results of ESS per second obtained from simulation experiments with a logistic regression model. Panel (a) exhibits results based on for-loop implementations, while panel (b) shows the vectorised versions. We stress that within each panel, the RWM, SMH, MH-SS and Tuna implementations are either all based on for-loops or all vectorised. Overall, comparing panels (a) and (b), we can see that the vectorised versions of SMH-1 and SMH-2 are significantly faster than their for-loop counterparts. For instance, for $d = 50$ and $n = 10^5$, the efficiency of SMH-1 and SMH-2 shows a 15- and 39-fold improvement, respectively, as their ESS per second jumped from 10^{-2} and $10^{-0.3}$ to $10^{-0.8}$ and $10^{1.3}$, respectively. Unsurprisingly, the gains in terms of run-times for the vectorised MH-SS are smaller, especially for MH-SS-2 with large n , as it requires smaller subsamples.

C.2 Empirical results of the optimal scaling for SMH

In addition to the optimal scaling results for MH-SS presented in Section 4.4, we also performed simulation experiments to find the optimal acceptance rate for the scalable Metropolis–Hastings algorithm (Cornish et al., 2019) in order to guarantee a fair comparison against MH-SS, Tuna and RWM in the Sections 5 and 6. This section presents the efficiency results for a set of values for the scaling parameter λ ranging from 0.1 to 4 with increments of 0.2. Our empirical analysis focuses primarily on the results of the vanilla SMH-1 and SMH-2, though we also show SMH’s efficiency when equipped with the bounds introduced in Section 4.2 (i.e., SMH-NB).

As stated in Section 4.4 and now displayed in panel (e) of Figure 10, SMH-2 has an optimal scaling around that of the RWM, which in turn leads to an acceptance rate close to 0.234 (panel (c)). Panel (e) also displays that all algorithms, except SMH-1 and SMH-1-NB, have similar acceptance rates as a function of the scaling parameter, λ . For these algorithms, we find that the scaling must decrease more quickly with dimension than ℓ/\sqrt{d} to maintain a reasonable acceptance rate as dimension increases. For SMH-1, however, we found that the optimal acceptance rate is less obvious. For example, for synthetic data generated from a logistic regression with $n = 100,000$ and $d = 100$, panel (a) of Figure 10 suggests that acceptance rates from 8% to 20% maximise SMH-1’s efficiency. However, we observed in other experiments, not shown here for brevity, that the relation between efficiency and optimal acceptance rate might change as n and d vary.

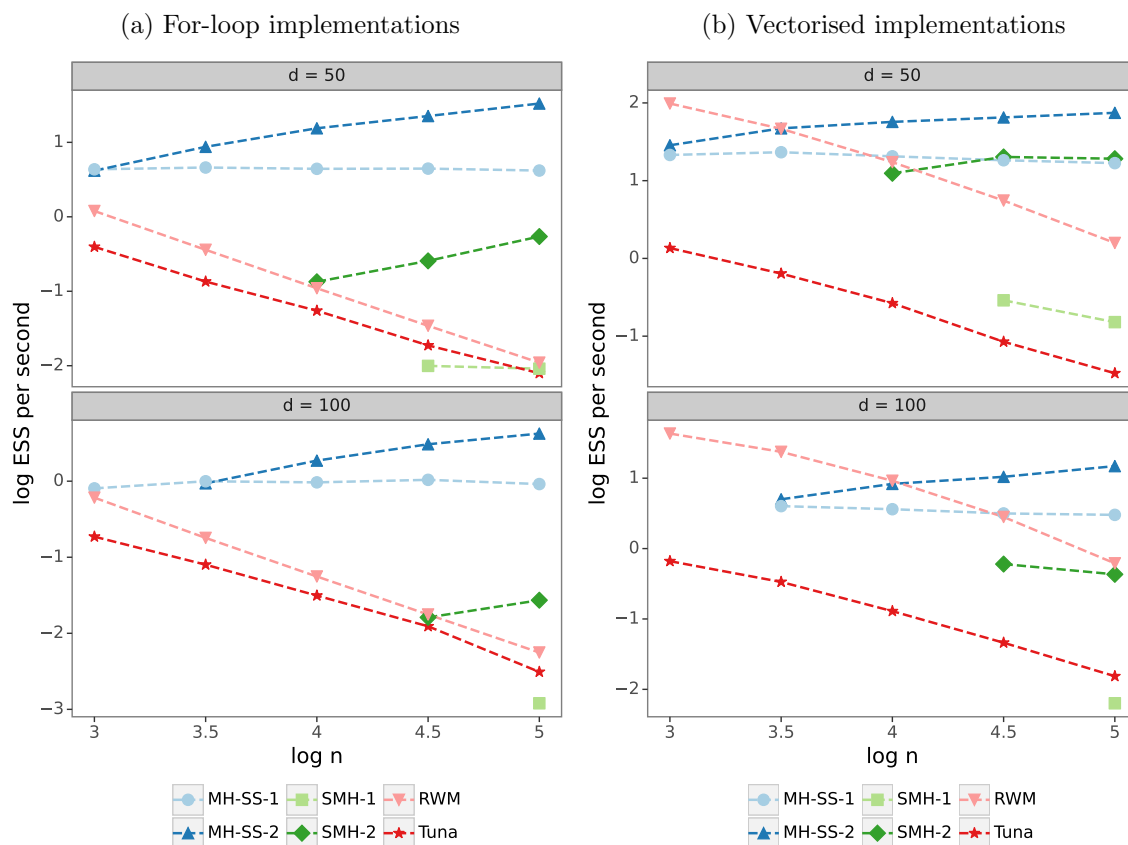


Figure 9: ESS per second for SMH and MH-SS on a logistic regression model. Except for the RWM, all algorithms have either for-loop-based implementations (panel(a)) or are all vectorised (panel (b)). Both axes are presented in the logarithm base 10. Some ESSs are omitted because $\mathbb{E}(B) \geq n$, which implies the use of the RWM algorithm.

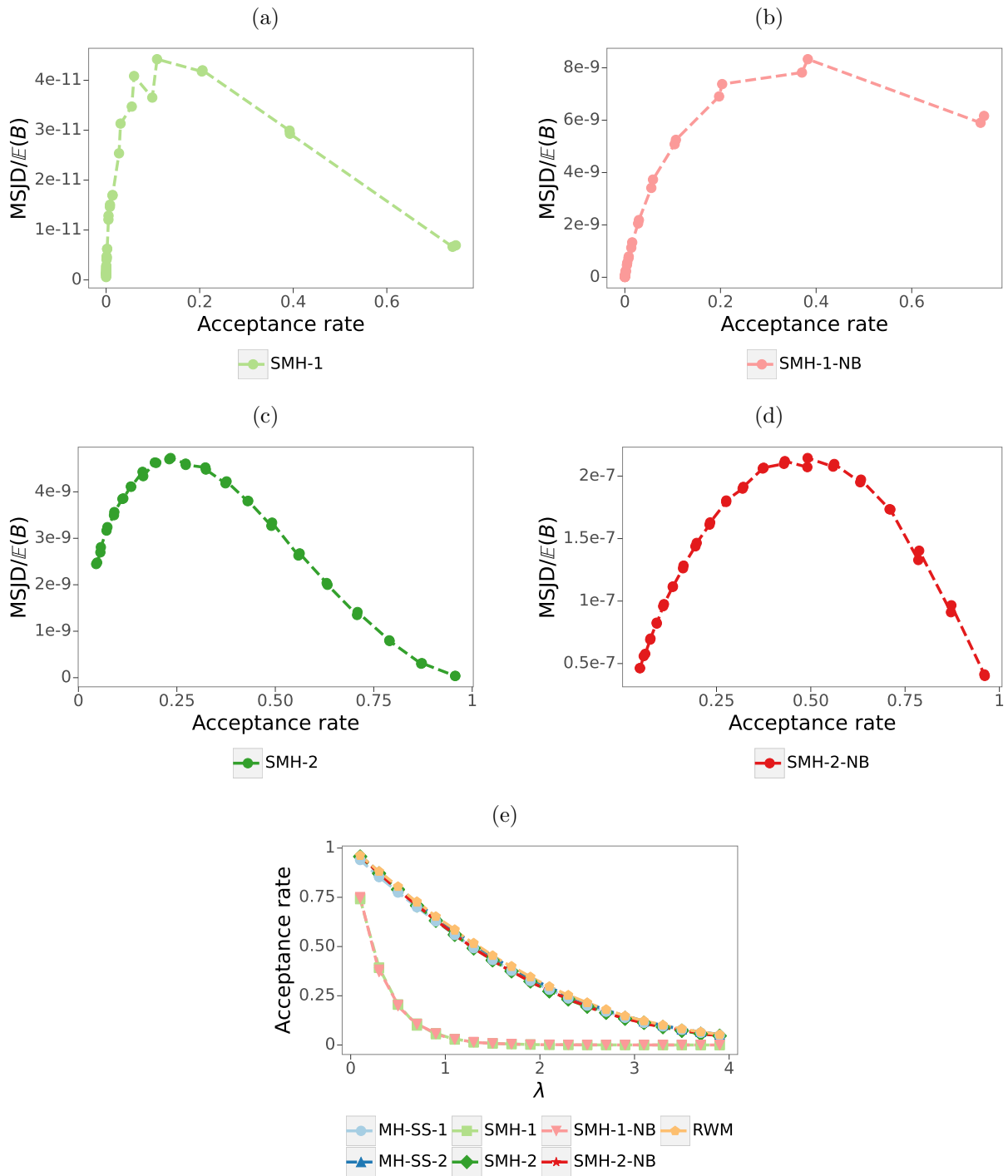


Figure 10: Acceptance rates and mean squared jumping distance (MSJD) over average batch size ($\mathbb{E}(B)$) based on a simulation experiment with a logistic regression model with dimension $d = 100$ and $n = 100,000$.

Table 6: Values of the hyperparameter χ in the Tuna algorithm used in the experiments of Section 3 considering $n = 31, 622$.

d	χ	λ
5	$1e^{-3}$	0.03
10	$5e^{-4}$	0.04
20	$1e^{-4}$	0.06
30	$5e^{-5}$	0.065
40	$3e^{-5}$	0.08
50	$2e^{-5}$	0.09
60	$1e^{-5}$	0.1

C.3 Experimental details of the Tuna tuning hyperparameter

To aid reproducibility of the results in the paper, Tables 6 and 7 in this section present the values of the Tuna tuning parameter as well as scaling parameter λ following the heuristic proposed by Zhang et al. (2020).

D Justification of optimal-scaling Assumption 2

The use of first-order control variates, $r_i^{(1)}$, is equivalent to using the approximation

$$\log \hat{p}^{(1)}(y_{1:n}|\theta) := (\theta - \hat{\theta})^\top \sum_{i=1}^n g_i(\hat{\theta}) + c = (\theta - \hat{\theta})^\top \nabla \log p(y_{1:n}|\hat{\theta}) + c,$$

whereas the use of second-order control variates, $r_i^{(2)}$, is equivalent to

$$\log \hat{p}^{(2)}(y_{1:n}|\theta) := -\frac{1}{2}(\theta - \hat{\theta})^\top \left\{ \sum_{i=1}^n H_i(\hat{\theta}) \right\} (\theta - \hat{\theta}) + c \approx p(y_{1:n}|\theta),$$

for large n , by the Bernstein-von Mises Theorem.

If $\hat{\theta}$ is a reasonable approximation to the mode, then $\nabla \log \pi(\hat{\theta}) \approx 0$ (indeed, this would be one definition of a reasonable approximation). In the Bernstein-von Mises limit, $\|\theta - \hat{\theta}\|_2 = \mathcal{O}(n^{-1/2}d^{1/2})$, and it is straightforward to show that provided $\nabla \log p(y_{1:n}|\theta)|_{\hat{\theta}} = \mathcal{O}(n^{1/2})$, $\log \hat{p}^{(1)}(y_{1:n}|\theta') - \log \hat{p}^{(1)}(y_{1:n}|\theta) = \mathcal{O}(1)$, typically.

Implicit in the justification of (9) is that, from the moment generating function of $S_i \sim \text{Pois}(\phi_i)$,

$$\mathbb{E} \left[\left(\frac{\phi'_i}{\phi_i} \right)^{S_i} \right] = \exp \left[\phi_i \left(\frac{\phi'_i}{\phi_i} - 1 \right) \right] = \exp[\phi'_i - \phi_i] = \exp[\ell_i(\theta') - \ell_i(\theta) - r_i(\theta, \theta'; \hat{\theta})].$$

Thus, the acceptance ratio for $\alpha_{2,MHSS}(\theta, \theta')$ in (11) has an expectation of

$$\mathbb{E} \left[\exp \left\{ \sum_{i \in \mathcal{I}} S_i \{ \log \phi'_i - \log \phi_i \} \right\} \right] = \mathbb{E} \left[\prod_{i=1}^n \left\{ \frac{\phi'_i}{\phi_i} \right\}^{S_i} \right] = \frac{p(y_{1:n}|\theta')}{p(y_{1:n}|\theta)} \exp \left[- \sum_{i=1}^n r_i(\theta, \theta'; \hat{\theta}) \right].$$

Despite our best efforts, whether first- or second-order control variates are used, the upper bounds from Corollary 2 are typically very loose. As argued directly after the statement of the corollary, this is because in moderate to high dimensions, $\theta' - \theta$, $\theta - \hat{\theta}$ and $\theta' - \hat{\theta}$ are close to

Table 7: Values of the hyperparameter χ in the Tuna algorithm used in the simulation experiments of Section 5.

n	d	χ	λ
1,000	10	$1e^{-3}$	0.14
	30	$2e^{-4}$	0.21
	50	$6e^{-5}$	0.25
	100	$1e^{-5}$	0.35
3,162	10	$9e^{-4}$	0.08
	30	$2e^{-4}$	0.11
	50	$6e^{-5}$	0.15
	100	$1.5e^{-5}$	0.22
10,000	10	$2e^{-3}$	0.04
	30	$2e^{-4}$	0.06
	50	$6e^{-5}$	0.09
	100	$1.5e^{-5}$	0.12
31,622	10	$1e^{-3}$	0.025
	30	$1e^{-4}$	0.04
	50	$6e^{-5}$	0.045
	100	$1.5e^{-5}$	0.07
100,000	10	$1e^{-3}$	0.015
	30	$2e^{-4}$	0.02
	50	$5e^{-5}$	0.03
	100	$1.5e^{-5}$	0.04

perpendicular to most covariate vectors x_i . However, we cannot use this fact to obtain better bounds without $\mathcal{O}(n)$ effort at each iteration. Typically, therefore, $c_i M(\theta, \theta') \gg |\ell_i(\theta') - \ell_i(\theta) - r_i(\theta, \theta'; \hat{\theta})|$. With $\gamma = 0$, (5) and (6) tell us that $\phi_i = c_i M(\theta, \theta')(1 - \delta_i)$ and $\phi'_i = c_i M(\theta, \theta')(1 - \delta'_i)$ with $\delta_i = -\min[0, \Delta_i]/\{c_i M(\theta, \theta')\} \ll 1$ and $\delta'_i = -\min[0, \Delta'_i]/\{c_i M(\theta, \theta')\} \ll 1$. Again from the moment generating function of a Poisson ϕ_i random variable:

$$\mathbb{E} \left[(\phi'_i / \phi_i)^{2S_i} \right] = \exp \left[\frac{\phi_i'^2}{\phi_i} - \phi_i \right] \approx \exp [2\phi'_i - 2\phi_i] = \mathbb{E} \left[(\phi'_i / \phi_i)^{S_i} \right]^2,$$

where the approximation arises from a first-order Taylor expansion. Thus, to first order,

$$\mathbb{E} \left[\left(\prod_{i=1}^n \left\{ \frac{\phi'_i}{\phi_i} \right\}^{S_i} \right)^2 \right] = \mathbb{E} \left[\prod_{i=1}^n \left\{ \frac{\phi'_i}{\phi_i} \right\}^{S_i} \right]^2$$

and so $\text{Var} \left[\exp \left\{ \sum_{i \in \mathcal{I}} S_i \{\log \phi'_i - \log \phi_i\} \right\} \right] = 0$ to first order. Heuristically, this justifies the assumption that for large d and typical $\theta \sim \pi$,

$$\exp \left[\sum_{i \in \mathcal{I}} S_i \{\log \phi'_i - \log \phi_i\} \right] \approx \frac{p(y_{1:n} | \theta')}{p(y_{1:n} | \theta)} \exp \left[- \sum_{i=1}^n r_i(\theta, \theta'; \hat{\theta}) \right].$$

The above and the arguments about $\hat{p}^{(1)}$ and $\hat{p}^{(2)}$ that precede it then imply Assumption 2.